JGR Biogeosciences

RESEARCH ARTICLE
10.1029/2025JG009375

Self- and Electrodic-Potential Response to Hydrological and Biogeochemical Processes in the Soil-Tree Continuum

M. Dumont[1,2], X. Takver[3], K. M. Jarecke[4], R. Yilangai[4], L. Slater[5], E. B. Graham[6,7], H. R. Barnard[4], P. L. Sullivan[3], and K. Singha[1]

[1]Hydrologic Science and Engineering Program, Colorado School of Mines, Golden, CO, USA, [2]Institute of Earth Sciences, University of Lausanne, Lausanne, Switzerland, [3]College of Earth, Ocean and Atmospheric Sciences, Oregon State University, Corvallis, OR, USA, [4]Department of Geography, Institute of Arctic and Alpine Research, University of Colorado-Boulder, Boulder, CO, USA, [5]Department of Earth and Environmental Sciences, Rutgers University Newark, Newark, NJ, USA, [6]Biological Sciences Division, Pacific Northwest National Laboratory, Richland, WA, USA, [7]School of Biological Sciences, Washington State University, Richland, WA, USA

Abstract Forest sustainability is regulated by the interplay between water and biochemical fluxes within the soil–tree continuum. However, capturing the daily to seasonal interplay of these ecohydrological and biological processes remains a major challenge. Instrumentation is typically compartmentalized—soil, roots, or trunk—hindering a unified understanding of the continuum. Here, we explore the potential of passive electrical methods to concurrently track water and biochemical fluxes across the soil–tree interface. Self and electrodic potential, depending on electrode type, respond to water flow, chemical and thermal diffusion, and redox gradients. We propose an electro-hydro-biogeochemical conceptual model linking electrical potential generation to tree transpiration, water uptake, hydraulic redistribution, and soil respiration. Using electrical potential monitored within the soil and across the soil-root-trunk continuum at the H.J. Andrews Experimental Forest, Oregon, USA, during summer 2023, we tested this model via daily correlations with sap flow, soil moisture, and carbon dioxide. Despite disturbances caused by wildfire smoke, electrical signals revealed strong correlations with daily patterns and event-driven perturbations (e.g., wildfire smoke) of hydrological fluxes and biological activity in both trees and soil. Water fluxes emerge as the primary driver of self and electrodic potentials, with redox gradients also playing a significant role across the soil–tree continuum. This study presents a framework for using passive electrical methods as proxies for monitoring forest ecohydrological resilience.

Plain Language Summary The tree is connected to the soil through its root system, enabling continuous exchanges of water and nutrients essential for its growth. Understanding how these exchanges fluctuate throughout the day and across the growing season is key to studying forest health. However, current methods often fragment the soil-tree continuum, making it difficult to capture the full picture. In this study, we explored whether natural electrical signals—known as self and electrodic potentials—can serve as reliable proxies for water movement and biogeochemical reactions across the soil–tree continuum. We compared passive electrical measurements with standard observations of water moving through a tree by data known as sap flow, soil moisture, and carbon dioxide released by soil, or soil respiration. We found that daily patterns and event-driven fluctuations (e.g., wildfire smoke) in electrical potential are driven by the interplay between water transport from soil to tree, soil respiration, and tree-related biochemical processes. This study shows that passive electrical methods provide a simple, non-invasive way to monitor the dynamic interactions between soil and trees. They offer a promising new tool to track how forests respond to environmental stress and change.

Key Points:

- Geophysical monitoring of forest sustainability using the self-potential method
- Quantification of ecohydrological and biogeochemical processes interplay within the soil-tree continuum
- Impact of wildfire smoke on tree transpiration and soil respiration

Supporting Information:

Supporting Information may be found in the online version of this article.

Correspondence to:

M. Dumont,
marc.dumont@unil.ch

Citation:

Dumont, M., Takver, X., Jarecke, K. M., Yilangai, R., Slater, L., Graham, E. B., et al. (2026). Self- and electrodic-potential response to hydrological and biogeochemical processes in the soil-tree continuum. *Journal of Geophysical Research: Biogeosciences*, *131*, e2025JG009375. https://doi.org/10.1029/2025JG009375

Received 25 AUG 2025
Accepted 5 FEB 2026

Author Contributions:

Conceptualization: M. Dumont, E. B. Graham, H. R. Barnard, P. L. Sullivan, K. Singha
Data curation: M. Dumont, X. Takver, K. M. Jarecke, R. Yilangai, H. R. Barnard
Formal analysis: M. Dumont, X. Takver, K. M. Jarecke, R. Yilangai, L. Slater, H. R. Barnard, P. L. Sullivan, K. Singha
Funding acquisition: H. R. Barnard, P. L. Sullivan, K. Singha
Investigation: M. Dumont, X. Takver
Methodology: M. Dumont, L. Slater, H. R. Barnard, P. L. Sullivan, K. Singha
Project administration: H. R. Barnard, P. L. Sullivan, K. Singha
Supervision: K. Singha
Validation: M. Dumont, X. Takver, K. M. Jarecke, R. Yilangai, L. Slater,

1. Introduction

Water availability for trees is governed by the complex interplay of atmospheric demand (Hogg & Hurdle, 1997; Venturas et al., 2017), subsurface moisture dynamics in soil and rock (Brantley et al., 2007; Callahan et al., 2022), and physiological regulation (Affortit et al., 2024; Buckley, 2019; Carminati et al., 2013, 2016; Williams & de Vries, 2020). To understand forest resilience in response to climate-driven and environmental stressors—including wildfire (Abatzoglou & Williams, 2016), drought (Gosling & Arnell, 2016), pest outbreaks (Teshome et al., 2020), and sea level rise (Kirwan & Gedan, 2019)—it is essential to integrate concurrent observations of water fluxes across the soil, root, and trunk continuum with leaf-to-root physiological measurements and rhizosphere dynamics under diverse meteorological conditions. However, such above- and below-ground

E. B. Graham, H. R. Barnard, P. L. Sullivan, K. Singha
Visualization: M. Dumont, X. Takver
Writing – original draft: M. Dumont, K. Singha
Writing – review & editing: M. Dumont, X. Takver, K. M. Jarecke, R. Yilangai, L. Slater, E. B. Graham, H. R. Barnard, P. L. Sullivan, K. Singha

hydrologic and physiological measurements are rarely collected at the same time, inhibiting the ability to quantify how external changes trigger tree responses, and how these processes feedback on water availability and biogeochemical reactions.

Various sensors and approaches have been developed to measure water or biogeochemical fluxes of the soil-root-trunk compartments, which leads to fragmenting of this continuum. In terms of water fluxes, instrumentation exists to monitor soil moisture at the point scale, including time- or frequency-domain reflectometry (e.g., Ojo et al., 2015; Walker et al., 2004), neutron probes (Evett et al., 2009) and tensiometers (e.g., Campbell, 1988; Spaans & Baker, 1992). In the tree itself, water fluxes can be estimated using sap-flow measurements in the trunk (e.g., Marshall, 1958) or in the roots (e.g., Fernández et al., 2001), and indirectly using methods such as dendrometers (e.g., Sevanto et al., 2008). In terms of physiological response, the acquisition of a tree's ecological and physiological parameters relies on selective sampling of above- or below-ground parts of the tree (e.g., Peters et al., 2020). In the subsurface, soil-redox monitoring is used to track biogeochemical reactions (e.g., Mattila, 2024), CO_2 monitoring can capture soil and root respiration (Raich, 1998; Raich & Tufekciogul, 2000), and laboratory analysis can provide information on soil and soil-water geochemistry (e.g., Bowman et al., 2023; Cooper et al., 2022; DiDonato et al., 2024). This non-exhaustive list of methods cannot capture soil-root-trunk continuum complexity because they measure one part of the system; additionally, some measurements are labor-intensive. New approaches that allow us to capture key processes at the interfaces of the soil, root and trunk, and to make those measurements continuously over time may help us to map and measure process-based connections and feedbacks along the soil-tree continuum.

Geophysical methods may offer proxies for measuring water fluxes and biological processes beyond the point scale (Dumont & Singha, 2026; Loiseau et al., 2023). Electrical resistivity tomography has been used to quantify diel fluctuations in trunk water storage (Guyot et al., 2013; Harmon et al., 2021; Wang et al., 2016), or to image both soil and trunk water storage together (Attia al Hagrey, 2007; Mares et al., 2016). Although electrical resistivity monitoring largely does not capture biogeochemical processes, recent studies have demonstrated the potential of electrical or impedance spectroscopy methods to quantify root-wall thickness and root area (Ehosioke et al., 2023; Peruzzo et al., 2021), and to monitor root water uptake and root adaptation to stress (Cseresnyés et al., 2024). The operational complexity and current injection requirements of both resistivity and spectroscopy methods elevate maintenance needs and failure risk, hindering their applicability for long-term monitoring in remote environments.

Rather than inducing currents, passive methods that measure electrical potentials naturally occurring at or between electrodes can be used to look at a variety of processes. A commonly used passive electrical measurement is self-potential (SP), which uses two non-polarizing electrodes, thus avoiding electrical signals generated at the interface of the electrode by electrochemical reactions. SP has been used to quantify electrical potential induced by soil hydraulic potential occurring in forested systems (e.g., Voytek et al., 2019); however, measured voltages can also be generated by temperature (Hermans et al., 2014; Revil et al., 2016), ionic diffusion (Hu et al., 2020; Niu & McDavid, 2025), and redox gradients when electron conductors exist in the investigated medium (Guo et al., 2024; Revil et al., 2010). Another passive electrochemical measurement is electrodic potential (EP), where a metallic electrode is combined with a non-polarizing reference (Atekwana & Slater, 2009). EP measurement captures the tendency of electrochemical reactions to occur in the vicinity of the metallic electrode (Slater et al., 2008). This type of measurement has been used to monitor soil-redox reactions (Personna et al., 2008; Slater et al., 2008; Zhang et al., 2010) and sap flow in trees (Ghildiyal et al., 2025; Zapata et al., 2020). It is important to note that SP and EP do not investigate the same volumes and processes. SP non-invasively provides information on processes internal to the medium between the electrodes, while EP primarily captures the electrochemical state at the electrode.

SP and EP are sensitive to water fluxes, temperature variations, and chemical and redox gradients that make them a complementary tool to monitor both ecohydrological and biogeochemical processes. However, untangling the different processes controlling the electrical potential measured along the tree-soil continuum is difficult. Previous studies in the soil-vegetation continuum largely focus on the interpretation of electrical potential related to water fluxes (Hu et al., 2025; Loiseau et al., 2023; Voytek et al., 2019). Here, we explore the applicability of SP and EP in combination to look beyond water fluxes and record physiological responses of Douglas-fir (Pseudotsuga menziesii) to daily and seasonal changes. To achieve this goal, we seek to address two primary challenges: (a) developing a conceptual electro-hydro-biogeochemical model and (b) identifying appropriate protocols to monitor water fluxes and biogeochemical reactions using passive electrical methods.

2. Self- and Electrodic-Potential Monitoring of the Soil-Tree Continuum

2.1. Passive Electrical Method Theory

In the field, an electrical potential ($\Delta\varphi$, differences in voltage) is measured with a high-impedance voltmeter or datalogger between a reference, φ_{ref}, and a potential, φ_i, electrode such that:

$$\Delta\varphi = \varphi_i - \varphi_{\text{ref}}. \tag{1}$$

These measurements capture two types of potentials: (a) the electrodic potential (EP) induced by electrochemical reactions in the vicinity of the electrodes and (b) the self-potential (SP) related to the electric field naturally occurring in the medium between the two electrodes (Jougnot & Linde, 2013):

$$\Delta\varphi = \left(\varphi_i^{\text{SP}} + \varphi_i^{\text{EP}}\right) - \left(\varphi_{\text{ref}}^{\text{SP}} + \varphi_{\text{ref}}^{\text{EP}}\right). \tag{2}$$

In the following part, we present the theory of EP and SP as well as the type of electrodes used for passive-electrical measurements. The choice of electrode is critical, as SP measurements depend on non-polarizable electrodes to ensure a stable and identical electrodic potential at both ends of the measurement circuit such that only $\Delta\varphi^{\text{SP}}$ is measured.

2.1.1. Electrodic Potential

The EP of an electrode composed by the metal M is controlled by the ion-metal electrochemical equilibrium such as $M \leftrightharpoons M^{n+} + \text{ne}^-$, with M^{n+} defining the cations reacting with the metal, n the valence charge, and e^- the charge exchanged. For a single ion-metal pair, the modified Nernst equation can be used to estimate the EP at the metallic electrode, φ^{EP} (Jougnot & Linde, 2013):

$$\varphi^{\text{EP}} = \varphi_M^0 + \frac{k_B T_K}{\text{ne}_0} \ln\{M^{n+}\} \tag{3}$$

where φ_M^0 is the standard potential of the metal M within a solution with a concentration of M^{n+} at 1 mol-L^{-1} (mV); k_B is the Boltzmann constant (1.3806×10^{-23} J K^{-1}); T_K is the absolute temperature (K); e_0 is the elementary charge (1.6×10^{-19} C); and $\{M^{n+}\}$ is the ionic activity of the cation associated with the metal. For a composite metallic electrode, the overall EP results from the combination of the electrochemical potentials associated with each ion–metal pair.

2.1.2. External Current Sources

Self-potentials are induced by electrical fields, E (V m^{-1}), generated by current density sources, Js (A m^{-2}) from natural processes occurring inside the studied medium:

$$J = \sigma E + J_S \tag{4}$$

where σ is the bulk electrical conductivity of the medium (S m^{-1}). In natural environments, current density is related to four different sources: (a) electrokinetic (J_{EK}), (b) redox (J_{RD}), (c) electro-diffusive (J_{ED}) and (d) thermoelectrical (J_{TED}) (Figure 1). Below, we describe the mechanisms driving these four sources.

In a non-dry porous medium, the surface of all minerals is in contact with an aqueous solution. Under typical environmental pH conditions, there is often a negatively charged surface where some cations from the aqueous solution are weakly or strongly sorbed, forming the Stern layer. The sum of charge at the mineral surface, the Stern layer, and the outer diffuse layer is zero, creating an excess of charge, Q_v (C/m^3) in the diffuse layer (Figure 1a). This excess of charge is induced by the attraction of anions in the diffuse layer while cations are repelled in the free pore water. Water flows drag this excess of charge, inducing an electrokinetic source (Gindl et al., 1999; Revil & Jardani, 2013) that is proportional to the water flux vector, U (m/s):

$$J_{\text{EK}} = Q_v \times U. \tag{5}$$

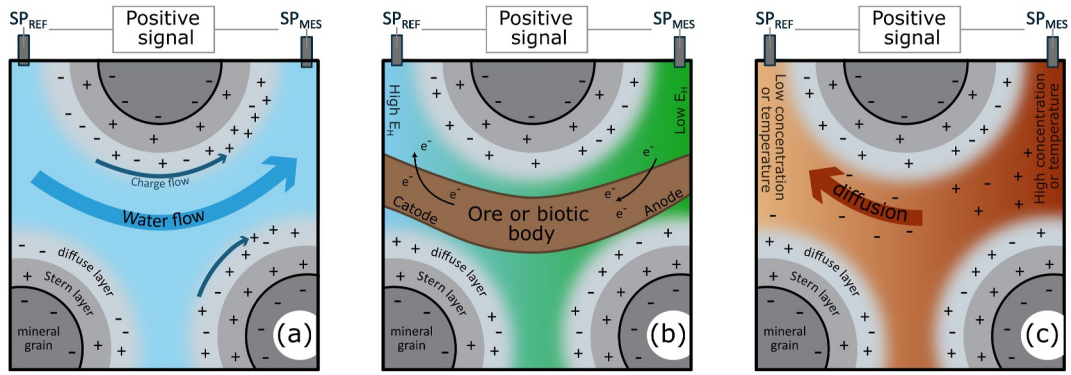

Figure 1. Schematic view of the four current-density sources generating a positive signal between a reference electrode (SP_{REF}) and a measurement electrode (SP_{MES}): (a) electrokinetic, (b) redox, and (c) electro-diffusive and thermoelectrical. The matrix is represented in dark gray with negative charges, the Stern layer in lighter gray with positive charges, and the diffuse layer in light gray. The sketch represents the conditions to generate a positive electrical potential with a reference at the left and the measurement electrode at the right. The (+) and (−) signs in the fluid represent cations and anions, respectively.

The excess charge depends primarily on the material's permeability (Jardani et al., 2007) and the degree of saturation in unsaturated settings (Soldi et al., 2018). Jougnot et al. (2012) provide more details about electrokinetic sources, including a mathematical formulation, and Hu et al. (2020) describe a case study modeling electrokinetic sources.

A current-density source called the redox source, often referred to as a geobattery, can be generated when an electron conductor (a mineral or a biotic conductor) crosses a strong redox gradient (Bigalke & Grabner, 1997; Sato & Mooney, 1960). Electrical potential has a reverse directionality to the redox potential (Arora et al., 2007; Figure 1b):

$$J_{\mathrm{RD}} \approx -\sigma \nabla E_h \tag{6}$$

where ∇E_h is the redox gradient between the reference and the measurement electrodes. This redox electrical potential can range up to a few hundred mV while electrokinetic sources produce signals of several tens of mV (Arora et al., 2007; Rittgers et al., 2013).

Third, electro-diffusion sources are generated by chemical gradients in the pore water. Chemical gradients induce diffusion from high-concentration to low-concentration areas (Figure 1c). Not all ions diffuse at the same rate; ions with smaller hydrated radii will diffuse more quickly than those with larger radii. Diffusion electrical potentials are generated if ions of opposing charge have differing diffusion rates and result in the unbalanced movement of charges. Anion- and cation-diffusion rates are captured by the Hittorf number, where $T_{(+)}$ is the macroscopic Hittorf number for cations and $T_{(-)}$ is the macroscopic Hittorf number for anions. The macroscopic Hittorf number corresponds to the fraction of electric charge carried by ions of the same polarity in the pore fluid, often due to differences in the ionic radius. The relative values of $T_{(+)}$ and $T_{(-)}$ determine the polarity of the source-current density defined as:

$$J_{\mathrm{ED}} = -\frac{k_B T_K}{e_0}\left(2T_{(+)} - 1\right)\nabla \ln a \tag{7}$$

where a is the pore-water activity. If $T_{(+)}$ is greater than 0.5, then J_{ED} is negative, while if $T_{(+)}$ is less than 0.5, J_{ED} will be positive (Revil et al., 2016).

The final current-density source is the thermoelectric effect, which refers to an electrical-potential gradient generated by a temperature gradient between two electrodes (Figure 1c). Cations and anions diffuse between high- and low-temperature regions (Revil et al., 2016). The thermoelectric effect is typically characterized by a thermoelectric coefficient ranging from −0.7 mV/°C to 1.4 mV/°C, with an average of 0.2 mV/°C (Zlotnicki &

Nishida, 2003). The magnitude of this coefficient depends on the fluid salinity and the grain size of the porous medium (Revil et al., 2016).

The four current-density sources have an additive contribution in the generation of electric current. We can then combine Equation 1 with the continuity equation, $\nabla \cdot J = 0$, to relate the potential difference measured in the field from the four source currents and the electrical conductivity of the ground:

$$\nabla \cdot (\sigma \nabla \varphi) = \nabla \cdot (J_{\mathrm{EK}} + J_{\mathrm{RD}} + J_{\mathrm{TED}} + J_{\mathrm{ED}}). \quad (8)$$

Because of the combined influence of these four distinct current-density sources, other supporting observations are needed to reliably disentangle the individual contributions of each process to the SP signal measured in the field.

2.1.3. Electrodes for Passive Electrical Measurements

Electrode choice critically determines the sensitivity of passive electrical methods to either EP or SP signals. When a metal electrode is in direct contact with the surrounding medium, it becomes sensitive to local electrochemical conditions and EPs are recorded. To prevent this sensitivity, the metallic wire of a non-polarizable electrode is immersed in an internal electrolyte housed in a plastic or ceramic tube, with external contact through a porous tip (Petiau, 2000). A measurement between two non-polarizable electrodes with identical electrolytes allows us to subtract out the EP component and only capture the SP signal. Nevertheless, electrolyte leakage or contamination, which modifies the internal electrochemical conditions of a non-polarizable electrode, has been reported by several studies (Hu et al., 2020; Jougnot & Linde, 2013), potentially leading to signal drift. For field monitoring, the electrolyte within the non-polarizable electrodes needs to be electrochemically stable over a long period of time, perhaps weeks to years. To ensure this condition, the electrolyte is typically mixed with mud or a gelling agent in a long electrode (10+ cm), limiting the electrolyte leaking or diffusion of ions within the electrode (Petiau, 2000). Installing long electrodes on trees is technically challenging given their size and maintenance requirements; metallic electrodes are better suited as they involve simpler deployment.

In the field, three configurations of passive electrical measurements are possible: (a) two metallic electrodes, where the measured signal mainly reflects the differential electrochemical state at each contact (φ_i^{EP}-$\varphi_{\mathrm{ref}}^{\mathrm{EP}}$); (b) one metallic and one non-polarizable electrode, which is primarily affected by the local electrochemical state at the metal electrode as the reference is considered stable over time (φ_i^{EP}); and (c) the use of two non-polarizable electrodes, which—assuming they remain electrochemically stable and identical—allows the measurement of SP signals (φ_i^{SP}-$\varphi_{\mathrm{ref}}^{\mathrm{SP}}$). In the first two configurations, both EP and SP signals are recorded, whereas the third configuration is designed to capture only the SP signal. We classify any measurement involving at least one polarizable electrode as an EP measurement, reflecting the dominance of the EP component while retaining SP contributions. Conversely, SP measurements employing two identical non-polarizable electrodes are specifically designed to remove the EP contribution and isolate the SP component.

2.2. A Soil-Root-Trunk Electro-Hydro-Biogeochemical Conceptual Model

This section presents a conceptual electro-hydro-biogeochemical model showing how passive electrical methods (SP and EP) can be used for monitoring key ecohydrological and biogeochemical processes in the soil-root-truck continuum (Figure 2a).

2.2.1. Hydrological Processes

The first current-generating process is water flow (Figure 1a), both in the tree and soil. Figure 2 During the day, tree transpiration drives the water potential gradient from the soil to the atmosphere that generates upward sap flow through the xylem tissue (Hölttä et al., 2006; Joshi et al., 2022; Figure 2a) while decreasing sapwood saturation and soil moisture around the root system; this process generates a water potential gradient in the soil (Figure 2b). When transpiration stops during nighttime hours, the tree-water uptake and sap flow continue to recharge the stem water deficit caused by daily transpiration until the water-potential gradient comes into equilibrium between the aboveground stem and belowground root system (Chen et al., 2018; Forster, 2014). When sap flow reaches a minimum, the water potential gradient in the soil could induce water flow through the

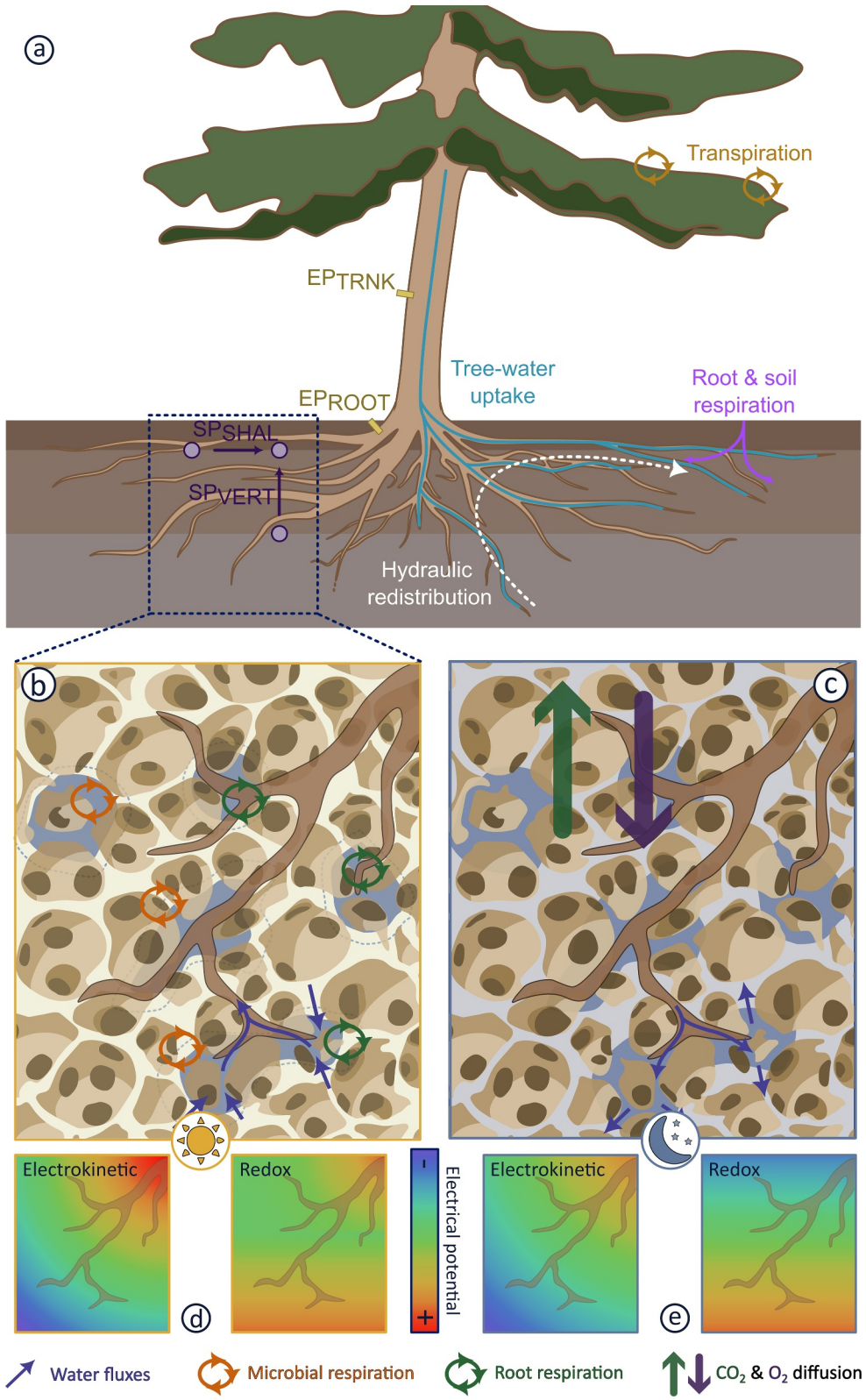

Figure 2.

root system. This passive flow, called hydraulic redistribution, may persist until increasing atmospheric demand at dawn exceeds the soil water potential gradient (Neumann & Cardon, 2012; Figure 2c).

Previous studies show that soil and tree water fluxes through porous media or tree and root xylem generate positive electrical potentials along the flow paths due to electrokinetic sources (e.g., Voytek et al., 2019 for soil fluxes and Zapata et al., 2021 for sap flow). In trees, the electrical potential, generally measured using a metallic electrode, is primarily related to the EP (hundreds of mV). The measured potential's temporal fluctuations may stem from internal water fluxes generating redox changes at the electrode–wood interface, or an electrokinetic source. During the day, tree-water uptake drives water movement from the soil to the leaves or needles, generating an excess of charge inducing an electrical field, extending from negative potentials in the soil to increasingly positive potentials along the upward flow path (Figures 2b and 2d). Consequently, daytime SP or EP signals should be positive when the reference electrode is placed downstream (e.g., deep in the soil) and the measurement electrode upstream (e.g., in the shallow soil closer to the root network or within the tree). At night, tree-water uptake is reduced, minimizing electrokinetic sources. However, hydraulic redistribution induces water flows from the root to the soil, which should generate negative SP signals in the electrode setup described before (from the root to the soil; Figures 2c and 2e). During the summer, declining sapwood saturation and increasing solute concentration are expected to modify the EP and SP signals associated with water flux, potentially generating a seasonal trend.

2.2.2. Redox Processes

Redox conditions along the soil-tree continuum are complex and have not been well-explored in the literature to date. Most of the limited studies using EP in trees focus on electrokinetic sources without considering the redox source (Hu et al., 2025; Zapata et al., 2020); however, redox gradients can generate a geobattery and EP signals (Figure 1). While EP is directly sensitive to redox-state variations at the measurement electrode, biogeobatteries can generate an SP signal if a metallic or biotic bridge allows electron movement. In trees, the plasma membranes and xylem play the role of a biotic conductor for internal tree redox reactions (Levengood, 1970; Tattar & Blanchard, 1976). Consequently, it is possible that root xylem or biofilms might create a biotic bridge for electron exchange between zones with different redox potentials across the soil-tree continuum, generating a biogeobattery (Fachin et al., 2012; Guo et al., 2024).

Physiological processes modify a tree's internal redox potential by generating biochemical reactions triggered by light, like photosynthesis, or by biotic and abiotic stresses, like systemic signaling (Miller et al., 2008). For example, in leaves or needles, photosynthesis is a high-rate redox metabolic process that generates reactive-oxygen species as natural byproducts (Dietz et al., 2016; Foyer & Noctor, 2005), but these variations in redox potential are located in the leaves and are naturally compensated by cellular homeostasis (Scheibe et al., 2005). Biotic and abiotic stresses trigger systemic signaling combining hydraulic (Christmann et al., 2007), redox (reactive-oxygen species; Miller et al., 2008), chemical (e.g., Ca^{2+}; Choi et al., 2014) and electrical signals (Szechyńska-Hebda et al., 2010) that may produce measurable voltages. Although systemic signaling has been primarily studied in the leaves of herbaceous plants, recent studies have captured these processes at the whole-plant scale (Choi et al., 2017; Peláez-Vico et al., 2022). In such cases, systemic signaling primarily travels through the phloem but can also influence xylem biochemistry, particularly through reactive-oxygen species-mediated pathways (Gaupels et al., 2017; Huber & Bauerle, 2016; Peláez-Vico et al., 2022; Ros-Barceló et al., 2006). Several studies have also demonstrated that electrical signaling can generate voltages up to 50 mV (Szechyńska-Hebda et al., 2010; Zimmermann et al., 2009) for a few seconds up to half an hour (Choi et al., 2014; Huber & Bauerle, 2016; Miller et al., 2008). As such, systemic signaling may generate electrical potentials due to the variations in the redox state of sap. These electrical potentials should mainly occur as high-frequency transient events without consistent diel patterns, while the other SP and EP signals likely have diel trends based on the model introduced throughout this section.

Figure 2. Conceptual electro-hydro-biogeochemical model of the soil-root-trunk continuum. (a) The four main ecohydrological processes and associated measurements explored here are: 1) photosynthesis, 2) tree-water uptake, 3) hydraulic redistribution, and 4) root and soil respiration. On the left of the tree, the proposed geophysical set-up is presented with SP electrodes in the soil, and EP electrodes in the root at the base of the tree and on the trunk. (b) A zoom in of soil-root processes during the day and (c) night highlights water fluxes, microbial and root respiration, and gas diffusion. A simplified representation of the voltage field in the soil generated by electrokinetic and redox sources (d) during the day and (e) night is represented in color.

In soil, redox potentials are generated by biogeochemical reactions such as soil respiration, which is driven by soil temperature as well as moisture in unsaturated conditions (Hanson et al., 2000). In natural soils, the redox potential spans a wide range, from high values under oxic conditions (where O_2 is the dominant electron acceptor) to low values under strongly reducing conditions (where CO_2 is reduced to methane; Husson, 2013). A primary process controlling soil CO_2 is heterotrophic respiration, which involves electron transfer to generate energy within living cells (Ben-Noah & Friedman, 2018). Soil heterotrophic respiration is the combination of root and microbial respiration, which together alters the soil redox potential (Hanson et al., 2000). The impact of soil respiration on soil redox depends on CO_2 diffusion toward the atmosphere, and oxygen renewal in the soil. The efficiency of these gas exchanges is influenced by soil depth, moisture content, and root architecture. In the upper soil, oxygen concentrations remain close to atmospheric levels (~20%) due to efficient exchange with the atmosphere. However, soil aeration—decreasing with depth—and increasing soil moisture reduces oxygen and CO_2 diffusion (Ben-Noah & Friedman, 2018), which leads to a progressive decrease in redox potential with depth (Zhang & Furman, 2021). Also, soil respiration is stronger near the root network due to the close coupling between root and microbial activity (Bond-Lamberty et al., 2004). The interconnection of root and microbial respiration, as well as the control of soil properties on gas diffusion, generate redox gradients in the soil during the day (Hanson et al., 2000; Figures 2d and 2e).

The diel pattern of soil respiration follows the transpiration rate with increased activity during the day, decreasing the soil's redox state (Figures 2b and 2d; Ben-Noah & Friedman, 2018). At night, reduced transpiration leads to decreased root respiration, allowing oxygen concentrations in the soil to increase, which raises the redox potential (Ben-Noah & Friedman, 2018; Husson, 2013; Zhang & Furman, 2021; Figures 2c and 2e). Thus, it can be inferred that soil respiration generates a negative redox gradient toward the center of the root system during the day. If the roots create biotic bridges along this negative redox gradient, this should induce a positive SP signal in the previously described electrode setup (Figure 2a).

Finally, the redox gradient between soil and root remains, to our knowledge, unexplored. Given that both microbial and root respiration consume oxygen and release CO_2, a local decrease in redox potential is expected with respiration. Root homeostasis may actively regulate a root's internal redox potential. This might generate a redox gradient between the more reduced soil (more negative potential) and the root (more positive potential). Such a redox gradient could induce a negative electrical potential difference between the soil and the root. During the night, the soil redox gradient, as well as the gradient between the soil and the root, increases as oxygen diffuses within the soil and the root system.

2.2.3. Thermoelectric and Electro-Diffusion Sources

The thermoelectric and electro-diffusion sources correspond to electrical potentials induced by ion movement generated by increased ion collisions due to higher chemical concentrations or temperature gradients, respectively. To be measured, ions need to move from the reference electrode to the measurement electrode within pore water in the soil and/or in the sap within roots or stems. In unsaturated soils, ion diffusion, which is controlled by the volumetric water content (VWC) and tortuosity (Tokunaga et al., 2017; Zhuang et al., 2024), is reduced at low soil-moisture content (Yang et al., 2024). Thus, ion diffusion generated by thermoelectric and electro-diffusion in unsaturated soils is unlikely to generate measurable electrical potentials between electrodes in the soil. Additionally, water fluxes and ion diffusion occur symplastically or via transmembrane processes in the trunk and roots (Javot & Maurel, 2002). Diffusion barriers exist to ensure a tighter control of water and solute fluxes in the tree (Nawrath et al., 2013), which should also limit the generation of electrical potential by electro-diffusion. In comparison, physiological processes such as systemic signaling induce cell-to-cell chemical waves, where the information passes from one cell to another without chemical diffusion (Peláez-Vico et al., 2022). We consequently suggest that the electrical potential generated from thermoelectric and electro-diffusion sources is small in comparison to the other two possible electrokinetic and redox sources.

2.2.4. Geophysical Monitoring of the Soil-Root-Trunk Continuum

We introduce a combined use of EP and SP measurements to monitor the coupled ecohydrological and biogeochemical dynamics of the soil–tree continuum, with the following working hypotheses.

- EP_{TRNK} and EP_{ROOT}, defined as the potential difference between a metallic electrode in the trunk or root and a non-polarizable reference in the soil, reflect both diel sap-flow variations and seasonal biochemical shifts near the electrode. By using a non-polarizable soil reference electrode, we prevent the measured signal from combining two EP contributions. As a result, EP_{TRNK} and EP_{ROOT} can be interpreted as the sum of the electrode's electrochemical potential and the SP signals between the soil and the trunk or the root, respectively.
- SP_{SHAL} and SP_{VERT}, based on measurements between shallow horizontal and vertical non-polarizable electrodes, are expected to reveal spatial patterns of root water uptake and may additionally respond to respiration-driven redox gradients—assuming the xylem or biofilms facilitate electron transport.

This dual monitoring strategy is designed to resolve the interplay between water fluxes and redox activity across temporal (daily to seasonal) and spatial (vertical/lateral) scales in the root–soil interface.

3. Field Experiment Methods

3.1. Study Site

We tested our electro-hydro-biogeochemical conceptual model at WS10 of the H.J. Andrews Experimental Forest in western Oregon, USA. Located in the Cascade volcanic range, the elevation of this 0.1 km^2 watershed spans from 480 to 565 m, with 27°–48° slopes (McGuire et al., 2007). The substratum is composed of andesitic tuffs and breccias with a weathering profile. At the surface, the soil is a Mesic Andic Humudepts, which covers a weathered saprolite layer (Harr & McCorison, 1979). After being clear cut in 1975, it was replanted with a Douglas-fir (Pseudotsuga menziesii) monoculture. The climate is Mediterranean with a wet winter; approximately 80% of the 2,220 mm of precipitation falls between October and April (McGuire et al., 2007). We instrumented four sites in the summer of 2023 to explore the replicability of the proposed geophysical monitoring methodology. A wildfire starting August 7th prevented any field maintenance until the fall; however, all of the SP and EP instruments were working correctly from installation on the July 10th until 31 August 2023, when they shut down due to the lack of solar power associated with smoke. Soil monitoring was limited by instrumental issues and only one factory-calibrated soil moisture, soil CO_2 and soil temperature instrument recorded data during the summer of 2023. Here, we present the results for sites with both geophysical and environmental monitoring, while the Text S1 in Supporting Information S1 presents the different sites and compares the replicability of geophysical monitoring.

3.2. Self- and Electrodic-Potential Monitoring

We used a Campbell CR1000 high-impedance datalogger to monitor electrical currents measured in the soil with Petiau Pb/$PbCl_2$ SP electrodes (SDEC PMS 9000, 180 mm in length; Petiau, 2000). Our setup measured potential differences between all single-ended electrodes and the reference electrode connected to the CR1000's ground. The reference SP electrode was installed vertically in the soil at depth of 120–130 cm and connected to the CR1000 ground to make single-ended measurements. Three other SP electrodes were installed horizontally, two near the surface at the limit between soil horizons O and A, and one at depth (120–130 cm) at the surface of the saprolite (Figure 2). On the tree, two stainless steel screws, 50 mm in length, were embedded into the trunk at the boundary between the bark and the sapwood to primarily measure EP signals and the potential SP contributions. The screws were located (a) on a major root, and (b) 2 m above the ground (Figure 2a). The screws were protected from the weather with liquid electrical tape. During the installation on the trunk, the bark and the living cambium were removed so that the screws could be inserted directly into the sapwood. The diameter at breast height (DBH) of the three trees is 27.9 cm, with an estimated sapwood thickness of 4.1 cm (according to the model presented in Lassen & Okkonen, 1969). The screw is therefore expected to be predominantly located within the sapwood, although the tip may extend slightly into the heartwood. We do not expect the tip entering the heartwood to influence the measured signal. Stainless screws are composed of different metals and the soil aqueous solution is composed of a mix of cations, making the estimation of EP signals related to the redox state difficult. Instead, we focus our interpretations on qualitative interpretations of the daily and seasonal variations.

Because we use single-ended electrodes, all measurements were made as a function of one reference electrode. Taking measurements with respect to one unique reference electrode speeds the deterioration of the internal electrochemical equilibrium of the reference, generating a systematic bias in all the measured potentials. To minimize this effect, we differenced out the reference electrode by subtracting the electrical potentials measured at two different electrodes, a and b, such that $SP = \varphi_a - \varphi_b$, with φ_a the electrical potential of the measurement

electrode, and φ_b the electrical potential of the new reference electrode. Using this equation, we calculate the two SP signals: SP_{SHAL} measured between two SP electrodes installed in the shallow soil at the interface between the O and A horizons, with the electrode farthest from the tree serving as the reference and the electrode closest to the tree as the measurement electrode; and SP_{VERT}, measured between two vertically aligned electrodes, with the deeper electrode serving as the reference and the shallower electrode as the measurement electrode (Figure 2a). EP signals were calculated using the deep SP electrode in the soil as a reference and the root EP electrode for EP_{ROOT} or the trunk EP electrode for EP_{TRNK} (Figure 2a).

3.3. Environmental Data Monitoring

We also monitored multiple environmental data on weather, tree, and soil hydro-biogeochemical variations to constrain our interpretations. We used weather time series to capture variations potentially impacting ecohydrological and biogeochemical processes. Because no weather station was installed in WS10 given the steepness of its slopes and the dense tree coverage, we used the precipitation, air temperature, solar radiation, air vapor pressure deficit (VPD), and wind speed from the H.J. Andrews PRIMET climatic station (Daly et al., 2025; Daly & Rothacher, 2025), which is located less than 1 km away from WS10 (Figure S4 in Supporting Information S1).

We used trunk and root sap velocity data as a proxy for the sap fluxes related to transpiration and tree-water uptake. We used a heat-ratio method based on heat-pulse velocity because of its ability to detect slow and reverse flows (Burgess et al., 2001). This method is based on temperature monitoring with two sets of thermocouples, one downstream and one upstream of the heating element connected to a CR1000 Campbell datalogger. The thermocouples, installed at 1.3 m above the ground, are 2.5 cm long with an inner and outer sensor 1 and 2.5 cm away from the cambium, respectively. The inner sensor sap velocity was processed to adjust the zero-flow offset using a double regression based on the lowest daily sap velocity over the entire length of the data with a 10-day moving window (Merlin et al., 2020). The sap velocity was further corrected using the wood and sap thermal properties using Burgess et al. (2001) equation. Sap velocity was not measured in the same trees as the EP signals to avoid any biogeochemical feedback from sap velocity instrumentation (stainless steel probes) and its heat pulse in EP signals. The tree instrumented for sap flow, located within 5 m of the EP tree, has a DBH of 30 cm. In Text S2 of Supporting Information S1, we demonstrate that the diel patterns of site-specific sap-flow measurements are consistent and that using any of these data would lead to the same interpretations.

To constrain subsurface ecohydrological processes, we installed CO_2, soil temperature, and soil moisture sensors (Figure S5 and S6 in Supporting Information S1). Soil moisture was used to constrain tree-water uptake and hydraulic redistribution, while soil CO_2 was used as a proxy of the root-soil respiration. We installed one Sentek Drill & Drop (Sentek Pty Ltd, Stepney, SA, Australia) soil moisture and temperature sensor, which collected data every 10 cm over 90 cm within 2 m of the monitored tree and the SP electrodes in the soil. Soil temperature and VWC sensors were installed between June 15th and 15 July 2023, and all the sensors were reinstalled on July 27th to improve the contact between the sensors and the soil and thus the quality of VWC monitoring. Finally, a CO_2 sensor (GMP252, Vaisala, Helsinki, Finland) was installed 20 cm deep and collected data from July 28th to August 31st. The location of environmental data is presented in Text S1 of Supporting Information S1.

3.4. Data Processing and Time Correlation Analysis

To analyze this multidisciplinary data set, we first standardized all variables to a consistent temporal resolution. Atmospheric and sap-flow measurements, originally recorded at 15-min intervals, were resampled to a 10-min frequency. We then applied a moving average with a seven-point window to smooth the data and remove high-frequency noise.

To test our proposed conceptual model, we developed a time-correlation analysis allowing us to assess correlation strength and potential time lags between geophysical and environmental time series. First, we remove the seasonal trend to ensure the stationarity of the time series. To do so, we estimate a linear trend and remove it from the data. Second, the range of variations and the units of environmental and geophysical data were different, so we applied z-score normalization to standardize each data set. For example, to calculate the z-score of $EP^{z,d}_{ROOT}$, we extract daily EP^{d}_{ROOT} data for each day d:

$$EP^{z,d}_{ROOT} = \frac{EP^{d}_{ROOT} - \mu_{EP^{d}_{ROOT}}}{\sigma_{EP^{d}_{ROOT}}}$$

where $\mu_{EP^{d}_{ROOT}}$ and $\sigma_{EP^{d}_{ROOT}}$ are the mean and standard deviation of the EP^{d}_{ROOT} daily data; the z and d superscripts stand for z-score and daily, respectively. The time correlation is evaluated using a Pearson correlation coefficient, its p-value, and the lag between the two time series. The lag values were not used to adjust or shift the data. They were solely employed to interpret the temporal relationship between the parameters.

4. Results and Discussion

Our conceptual electro-hydro-biogeochemical model was analyzed to test SP and EP signals across event-driven perturbations (e.g., wildfire smoke) and daily fluctuations. This multi-scale approach highlights the potential of SP and EP to capture both natural cycles and transient disturbances. The short duration of our data set restricts robust conclusions at the seasonal and yearly scales. The comparison of SP and EP monitoring at the four sites is presented in the Text S1 of Supporting Information S1 with identification of ecohydrological patterns in the Text S3 of Supporting Information S1.

4.1. Event-Driven Perturbations Analysis

The event-driven perturbations analysis aims to highlight SP and EP reliability to capture ecohydrological processes over the summer under typical conditions as well as following a wildfire that modified the solar radiation, inducing perturbations that affected multiple data streams starting on August 14th (Figure 3).

Sap velocities, both in the tree and root, were elevated until the wildfire smoke reached the site (Figure 3a). Sap velocity decreased on rainy days, for example, on August 4th and 5th, and after the smoke reached the site.

In the soil, the VWC at 10 cm depth gradually decreased over the season, showing a slight increase every night likely due to hydraulic redistribution (Figure 3b). During rainfall, the soil VWC decreased more slowly, as can be seen on August 5th and 6th. Diel cycling exhibited lower amplitudes on August 17th and 29th, which could be related to a decrease in tree-water uptake (Figure 3a) triggered by lower VPD. The soil respiration, monitored by CO_2 concentrations, showed notable fluctuations during the summer (Figure 3b); however, these variations became more sizable after the smoke arrived, with a maximum amplitude between August 14th and 17th, and a minimum between August 22nd and 24th (Figure 3b).

The tree EP_{TRNK} signal shows high absolute values, over 500 mV, which can be related to electrochemical effects at the metallic electrode (Figure 3c). Its diel pattern generally tracks tree sap flow in terms of daily timing (Figures 3a and 3c), increasing in the early morning and decreasing in the afternoon. While this behavior seems to be driven by electrokinetic signals generated by sap flux, it could also partially result from diel changes in sapwood electrodic potential due to variations in moisture and electrical conductivity in the trunk (e.g., Harmon et al., 2021) or tree internal biological activity. Such hypotheses are supported by Hu et al. (2025), who decomposed an EP signal using variational mode decomposition. They reported an SP signal driven by sap flow that shows a diel pattern and amplitude distinctly different from the diel variations observed in the EP signal. At the seasonal scale, the EP_{TRNK} signal exhibits a notable increase, especially after the wildfire started, that is not observed in the sap-velocity data. This behavior may result from biochemical reactions in the trunk, variations in sapwood moisture, and consequent changes in tree electrical conductivity throughout the season that could modify the redox state at the metallic electrode. With complementary measurements—such as sapwood moisture and tree electrical conductivity time series—these EP_{TRNK} trends could potentially be linked to tree physiological stress responses.

The root electrical potential, EP_{ROOT}, exhibits an inverted diel pattern relative to root sap velocity (Figures 3a and 3c) and consistent with soil CO_2 concentration (Figure 3b). During the day, root respiration should decrease the redox state of the root, inducing a drop of EP_{ROOT} according to our conceptual model. Water flows from the soil to the root should generate a positive electrical potential. Consequently, daily variations of EP_{ROOT} might not be related to an electrokinetic source. The link between root respiration/CO_2 and EP_{ROOT} becomes particularly evident following the arrival of wildfire smoke at the site: CO_2 soil levels decrease until August 23rd, then rebound, and EP_{ROOT} exhibits an inverse pattern (Figure 3b).

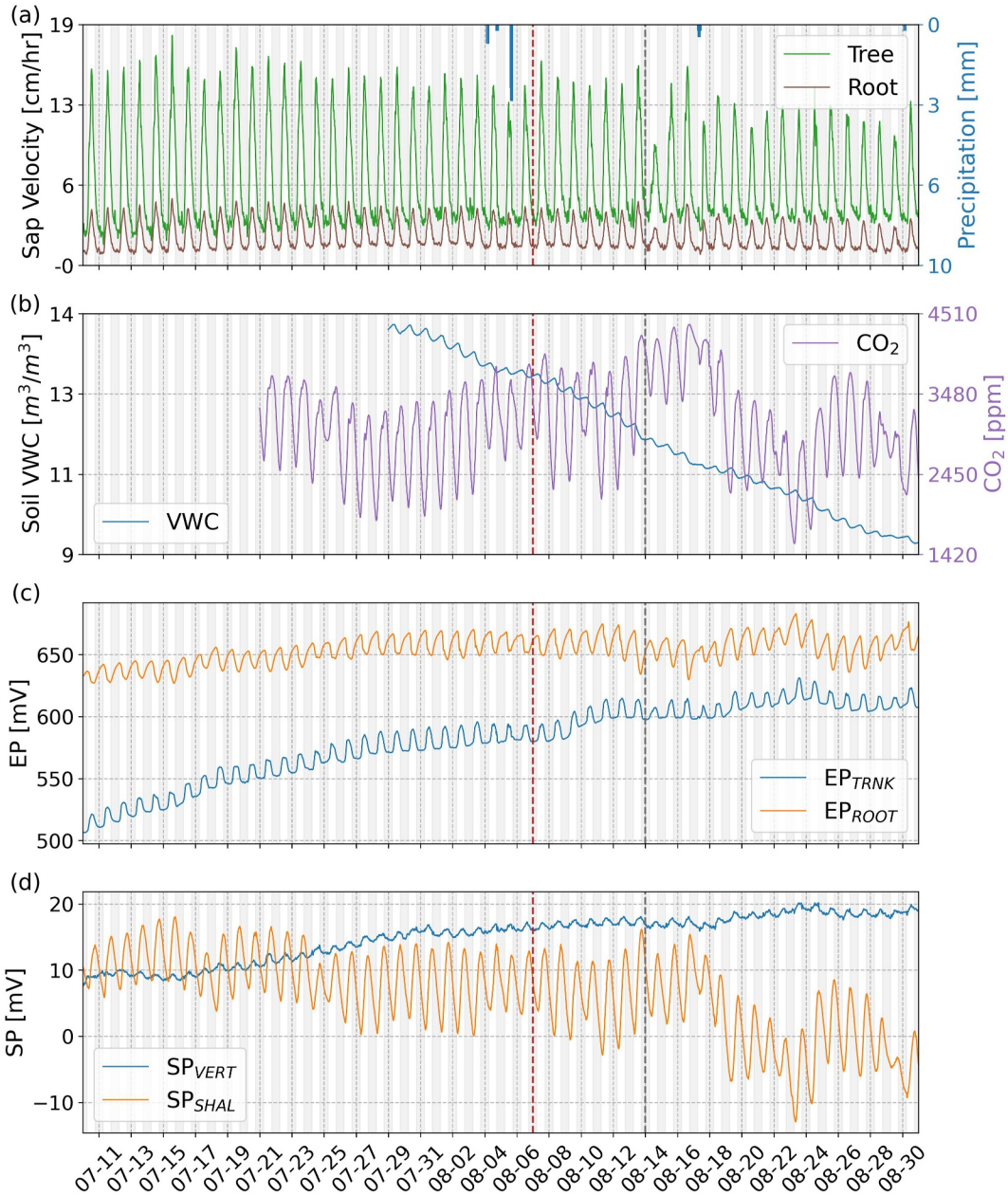

Figure 3. Time-series data from July 10th to 31 August 2023 for (a) tree and root sap velocity and precipitation; (b) soil volumetric water content and CO_2; (c) EP_{TRNK} and EP_{ROOT}, and (d) SP_{VERT} and SP_{SHAL}. The dashed dark-red vertical line corresponds to the start of the wildfire on August 7th, and the dashed gray vertical line is when the wildfire smoke starts to impact the study site (August 14th). In such dry conditions, small rainfall events (<5 mm) did not generate measurable infiltration. Much of the water was likely captured by the vegetation, making it impossible to capture infiltration with soil moisture or SP sensors.

The shallow SP_{SHAL} measurement appears to be responsive to diel variations of both soil VWC and CO_2 concentrations (Figure 3b). During the day, SP_{SHAL} and CO_2 increased, while the soil VWC decreased. SP_{SHAL} might be related to the addition of both electrokinetic and redox source, which could explain the large diel variations (±5–12 mV). When the wildfire smoke reached the site, both SP_{SHAL} and CO_2 variations followed the same trend: a quick decrease followed by a rebound, enhancing the potential of the redox source (Figure 3b).

During the day, when soil VWC decreased, SP_{VERT} increased, consistent with tree-water uptake variations (Figures 3b and 3d). During the night, SP_{VERT} decreased as tree-water uptake stopped. Over the summer, while

soil VWC declined, the SP_{VERT} signal increased. Conceptually, this trend could have been explained by an increase in tree-water uptake except that sap velocity decreased over the summer (Figure 3a), so transpiration does not explain our data. Instead, the decrease in soil VWC throughout the season likely increased the electrokinetic excess charge (Soldi et al., 2018), consequently amplifying the electrokinetic potential generated by water fluxes.

The response of SP and EP signals to wildfire smoke offers useful evidence for validating the monitoring of the soil–tree continuum. Water-flux-related signals (EP_{TRNK} and SP_{VERT}) exhibit only a modest decrease under smoke exposure, consistent with sap-flow and soil moisture observations. In contrast, signals sensitive to biological processes (EP_{ROOT} and SP_{SHAL}) show pronounced variability that aligns with CO_2 measurements. This differential sensitivity reinforces our interpretation of SP and EP data. It also suggests that wildfire smoke affects biological activity more strongly than hydrological fluxes within the soil–tree continuum. While these results suggest that EP and SP are qualitatively sensitive to the soil-tree continuum processes, we aimed to quantitatively explore the main processes generating each electrical potential measured. SP and EP signals result from the superposition of electrodic potential and external current sources (electrokinetic and redox sources); however, some processes may dominate in certain systems at certain times. Consequently, we use a time-correlation analysis to identify which processes occur simultaneously with the observed SP and EP signals, allowing us to eliminate those that are lagged as primary contributors. If SP or EP signals correlate strongly with only one process, it would allow us to hypothesize that this process is the primary source of the observed electrical potential.

4.2. Tracking Sap Flow With EP_{TRNK}

The electrochemical state in the trunk, $EP^{z,d}_{TRNK}$, has a strong correlation through time with the tree sap velocity, with a lag of 33 min (Figure 4a). In the morning, when transpiration begins, we see an increase in $EP^{z,d}_{TRNK}$; this process naturally reverses around midday. $EP^{z,d}_{TRNK}$ is also strongly correlated with the root sap velocity with a lag of 27 min (Figure 4b). $EP^{z,d}_{TRNK}$ is not temporally correlated with soil moisture (Figure 4c) or CO_2 (Figure 4d), which suggests that this electrical potential is not generated by soil respiration and soil moisture fluxes; this result perhaps makes sense given that the metallic electrode is in the tree trunk. In absence of other processes able to generate significant current, we suggest that $EP^{z,d}_{TRNK}$ largely captures trunk and root sap flow. However, we cannot exclude that biochemical reactions driven by water and solute fluxes in the tree may affect the amplitude of $EP^{z,d}_{TRNK}$.

4.3. Capturing Tree-Water Uptake and Soil Hydraulic Redistribution Using SP_{VERT}

$SP^{z,d}_{VERT}$ is expected to be sensitive to processes happening vertically in the soil. The correlation between $SP^{z,d}_{VERT}$ and tree and root sap velocity is weaker than $EP^{z,d}_{TRNK}$ (Figures 5a and 5b), with lags over an hour long. During the morning, $SP^{z,d}_{VERT}$ increases simultaneously with both root and tree sap velocity (Figures 5a and 5b); however, at mid-day, $SP^{z,d}_{VERT}$ stays higher longer than sap velocity, and keeps decreasing after both tree and root sap flows cease. $SP^{z,d}_{VERT}$ is weakly correlated with the soil moisture content (Figure 5c), which might be related to differences in scale given that SP integrates electrical potential over the meter scale and the soil-moisture probe measures VWC at the point scale at 10 cm depth. Also, $SP^{z,d}_{VERT}$ does not seem impacted by soil rewetting during the night (between 10p.m. and 4a.m.) Two hypotheses could explain this low correlation: (a) hydraulic redistribution occurs mostly in the first 20 cm of soil (Figure S6 in Supporting Information S1), which is a small fraction of the soil investigated by $SP^{z,d}_{VERT}$ measurements, and thus the electrical potential generated might be too small compared to the volume of soil investigated to be measurable, or (b) hydraulic redistribution might generate horizontal flows (Nadezhdina et al., 2010), which generate horizontal electrical potentials not captured by $SP^{z,d}_{VERT}$. The time correlation with CO_2 is also weak (Figure 5d), limiting the possibility of a redox source. In summary, $SP^{z,d}_{VERT}$ signal appears to primarily reflect daytime tree water uptake.

4.4. Monitoring Soil Respiration With SP_{SHAL}

The $SP^{z,d}_{SHAL}$ electrodes are located at the interface between O and A soil horizons, where respiration is stronger due to higher temperature variations and oxygenation. It is also at 10–20 cm depths that hydraulic redistribution has been captured by our soil-moisture measurements (Figure S5 in Supporting Information S1). Electrical

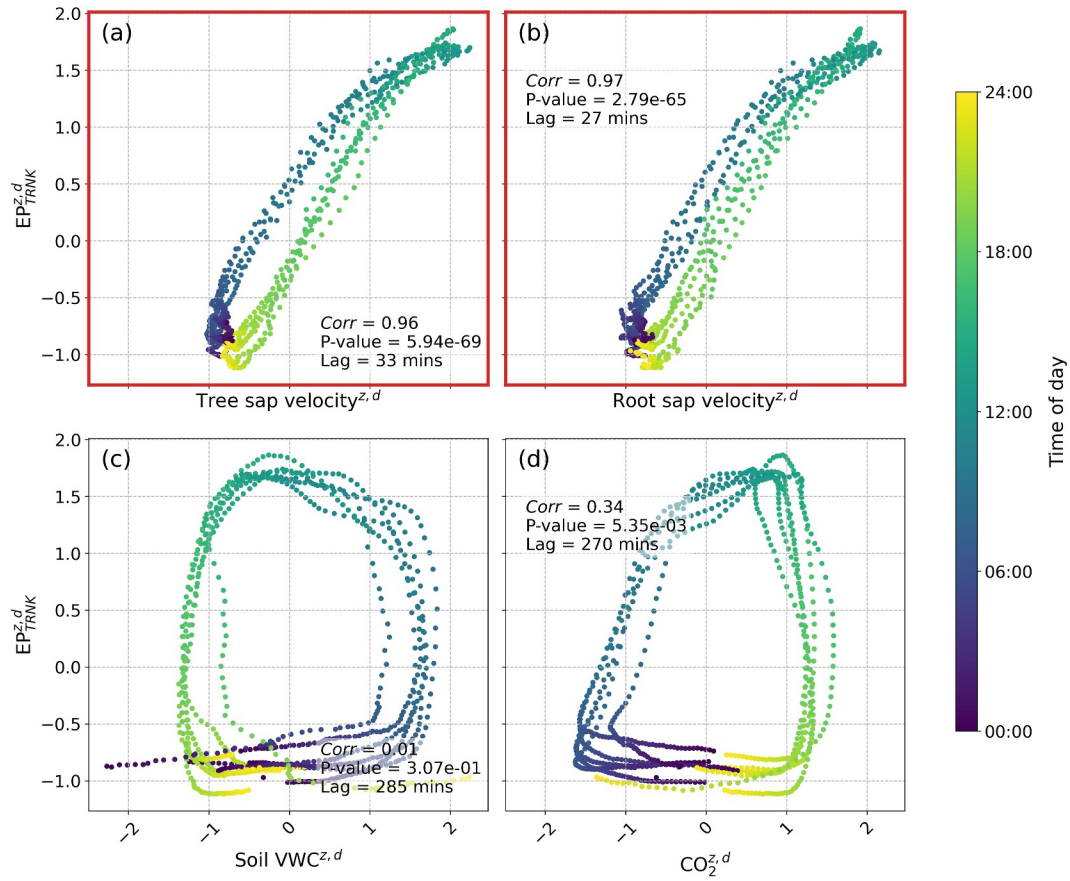

Figure 4. Daily correlation scatter plots of $EP^{z,d}_{TRNK}$ with (a) tree sap velocity, (b) root sap velocity, (c) soil water content, and (d) CO_2. The z-scored data presented here are unitless. The most significant time correlations are highlighted by red border. Seasonal trends were removed from the data using a linear regression, and the data were then averaged weekly and normalized with a z-score to focus on the daily dynamics.

potential measured by $SP^{z,d}_{SHAL}$ is not correlated with tree sap velocity (Figures 6a and 6b). The SP signal increases during the day, while sap velocity increases in the morning and decreases in the afternoon. Conversely, $SP^{z,d}_{SHAL}$ is strongly time correlated with both the soil moisture and the CO_2; during the morning, $SP^{z,d}_{SHAL}$ increases while the soil VWC decreases and the CO_2 increases (average lag 27 and 57 min respectively; Figures 6c and 6d). The strong relationship with soil VWC suggests that a part of $SP^{z,d}_{SHAL}$ signal is generated by electrokinetic sources from soil-moisture fluxes, despite low correlation with sap flow (Figures 6a–6c). But $SP^{z,d}_{SHAL}$ is also correlated with CO_2, suggesting a potential redox source from soil respiration (Figure 6d). These two strong time correlations suggest a cumulative SP signal that could explain the large diel variations of the $SP^{z,d}_{SHAL}$ signal (±5–12 mV; Figure 3c). The combination of soil SP and EP measurements may be a solution to disentangle water fluxes and soil respiration in the future. In addition, the difference in response between $SP^{z,d}_{VERT}$ and $SP^{z,d}_{SHAL}$ might highlight the complexity of soil water fluxes induced by tree-water uptake. Tree-water uptake may principally generate lateral fluxes in the shallow part of the soil.

4.5. Exploring Root Respiration With EP_{ROOT}

The electrochemical state measured in the root, $EP^{z,d}_{ROOT}$, shows a weak correlation with both the tree and root sap velocity (Figures 7a and 7b), suggesting that $EP^{z,d}_{ROOT}$ is not related to tree and sap flow. Indeed, sap flow should generate a positive electrokinetic potential along the water flow pathways from the soil to the root. $EP^{z,d}_{ROOT}$ starts

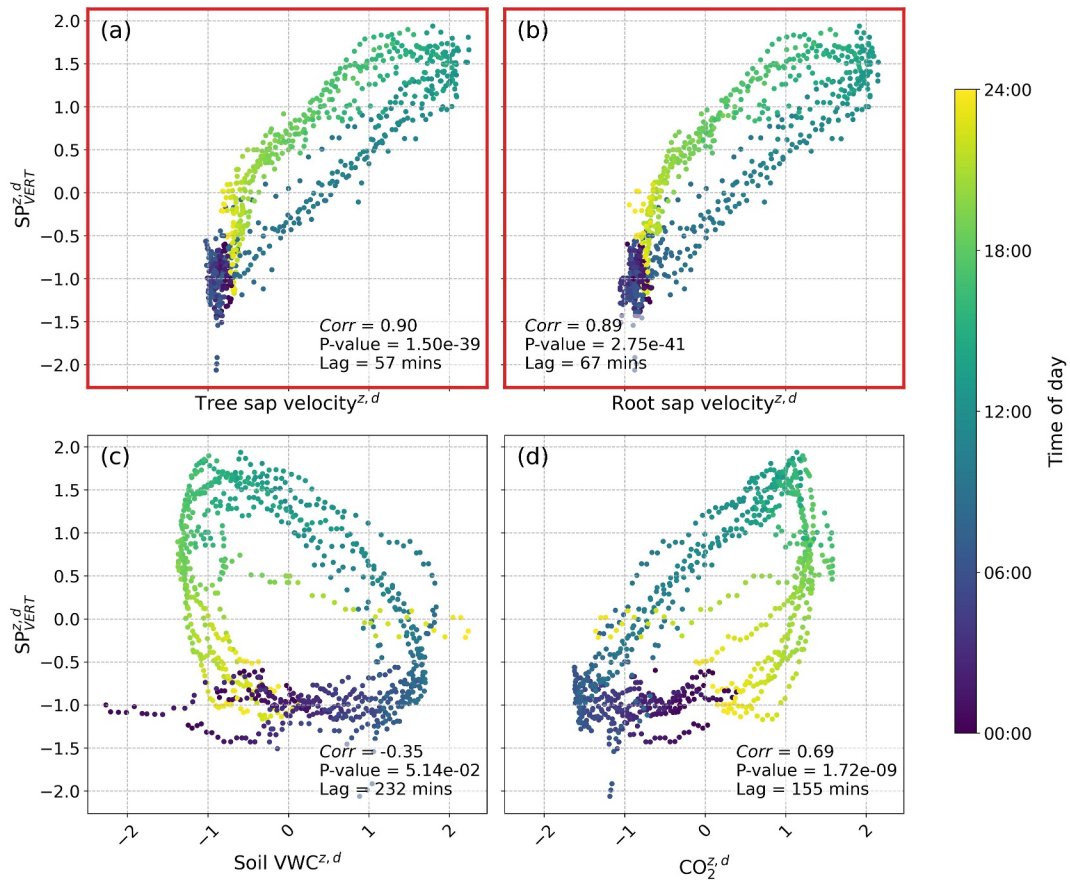

Figure 5. Daily correlation scatter plots of $SP_{VERT}^{z,d}$ with (a) tree sap velocity, (b) root sap velocity, (c) soil water content, and (d) CO_2. The z-scored data presented here are unitless. The most significant time correlations are highlighted by red borders. Seasonal trends were removed from the data using a linear regression, and the data were then averaged weekly and normalized with a z-score to focus on the daily dynamics.

to increase before the sap flow begins and then decreases during the day while the sap flows increase. During the night, $EP_{ROOT}^{z,d}$ increases while sap velocity is minimal.

However, $EP_{ROOT}^{z,d}$ is significantly correlated with soil VWC (average lag 110 min; Figure 7c); we see an increase in soil moisture simultaneously with the increase of electrical potential between the soil and the root. $EP_{ROOT}^{z,d}$ is also negatively correlated with the CO_2 in the soil (average lag 45 min; Figure 7d). The strong correlation with CO_2 data supports the hypothesis that soil respiration is the main contributor of the $EP_{ROOT}^{z,d}$ signal. This result suggests that the redox potential within the root decreases more than at the deeper reference electrode during the day, consistent with higher respiration rates near the surface compared to those a meter below the surface, where the reference electrode is installed. However, the correlation between the soil VWC drops due to tree-water uptake and the decrease of $EP_{ROOT}^{z,d}$ cannot be related to an electrokinetic source. Tree-water uptake should generate water flows from the soil to the root, which would be expected to increase $EP_{ROOT}^{z,d}$, while the opposite is observed (Figure 7c). Two hypotheses could explain this time correlation: (a) soil moisture controls microbial activity and related redox-potential variations (e.g., Miele et al., 2023) or (b) there is a co-evolution of ecohydrological processes without direct causation.

5. Conclusion and Perspectives

In this study, we propose a conceptual electro-hydro-biogeochemical model of the soil-tree continuum that integrates electrical potentials generated by EP and SP. We tested this model with ecohydrological and geophysical data monitored during summer 2023 to estimate the ability of SP and EP methods to capture daily ecohydrological

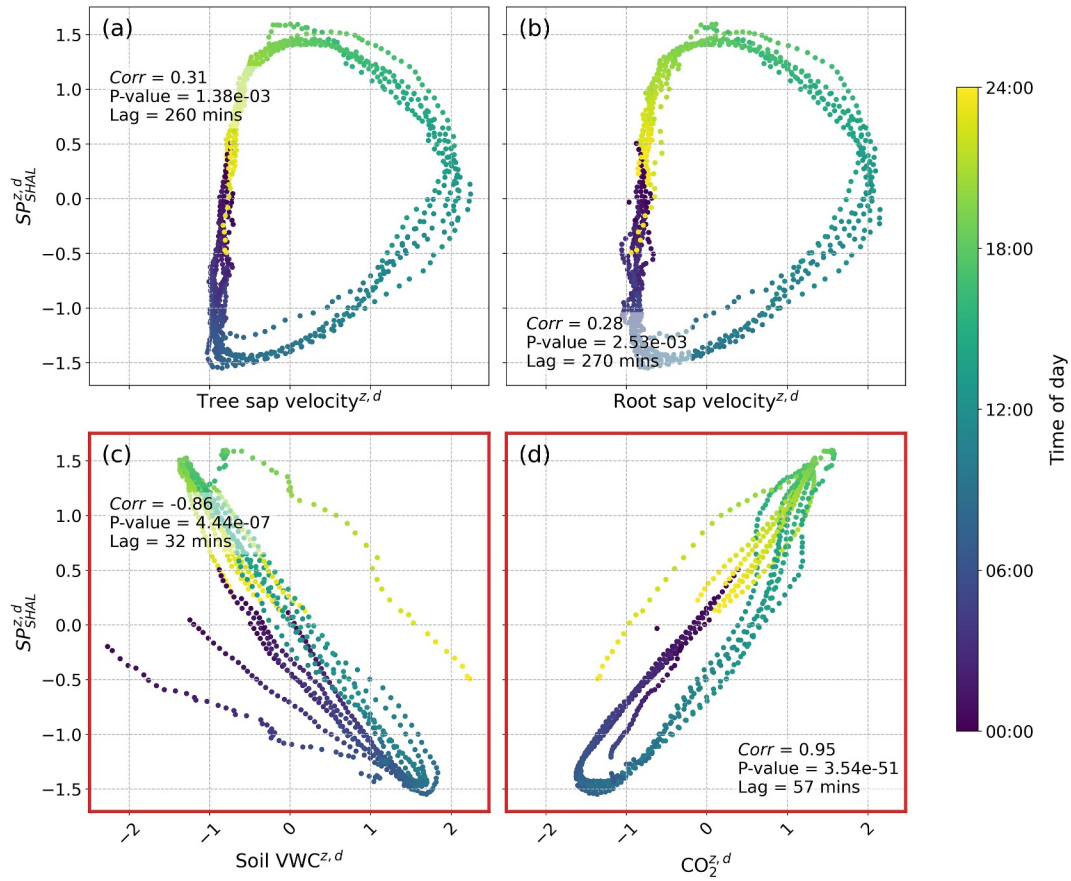

Figure 6. Daily correlation scatter plots of $SP_{SHAL}^{z,d}$ with (a) tree sap velocity, (b) root sap velocity, (c) soil water content, and (d) CO_2. The z-scored data presented here are unitless. The most significant time correlations are highlighted by red borders. Seasonal trends were removed from the data using a linear regression, and the data were then averaged weekly and normalized with a z-score to focus on the daily dynamics.

patterns and multi-day variations induced by climatic perturbations (e.g., wildfire smoke). Our objective is to highlight the potential of geophysics for high-frequency monitoring of water flux and biochemical reactions in the soil-tree continuum, recognizing notable complexities in interpretation of these data. This work is a first step in using such data in these systems and parsing the resultant signals.

To identify the ecohydrological and biogeochemical processes controlling electrical potentials in the soil-tree continuum, we identified time correlations between geophysical and environmental time series and related them with well-known processes. In the tree, we find that EP_{TRNK} is most strongly correlated with sap velocity, whereas at the root-level EP_{ROOT} data are more related to soil respiration. In the soil, SP_{SHAL} responds to both tree water uptake and soil respiration. Analysis of SP_{VERT} seems controlled by the tree-water uptake process, but its interpretation is difficult as it connects the shallow and deeper soils, where diel and seasonal patterns of soil water and respiration are different. The recurrence of these signal patterns across the four sites (Text S1 in Supporting Information S1), regardless of their distinct ecohydrological behaviors, supports the method's robustness and potential for broader application in tracking water fluxes and biogeochemical processes within the soil–tree continuum.

A key limitation of our study is the relatively short duration of the data set. Although we evaluate geophysical measurement performance in capturing ecohydrological processes, including daily patterns and responses to disturbances such as wildfire smoke, the observation period is too short to robustly assess seasonal dynamics and long-term monitoring reliability. Nevertheless, previous studies have demonstrated that SP electrodes can monitor soil water fluxes for at least a year (Hu et al., 2020; Voytek et al., 2019). Although EP measurements in trees are more recent, year-long deployments have also been documented (e.g., Hu et al., 2025). The primary

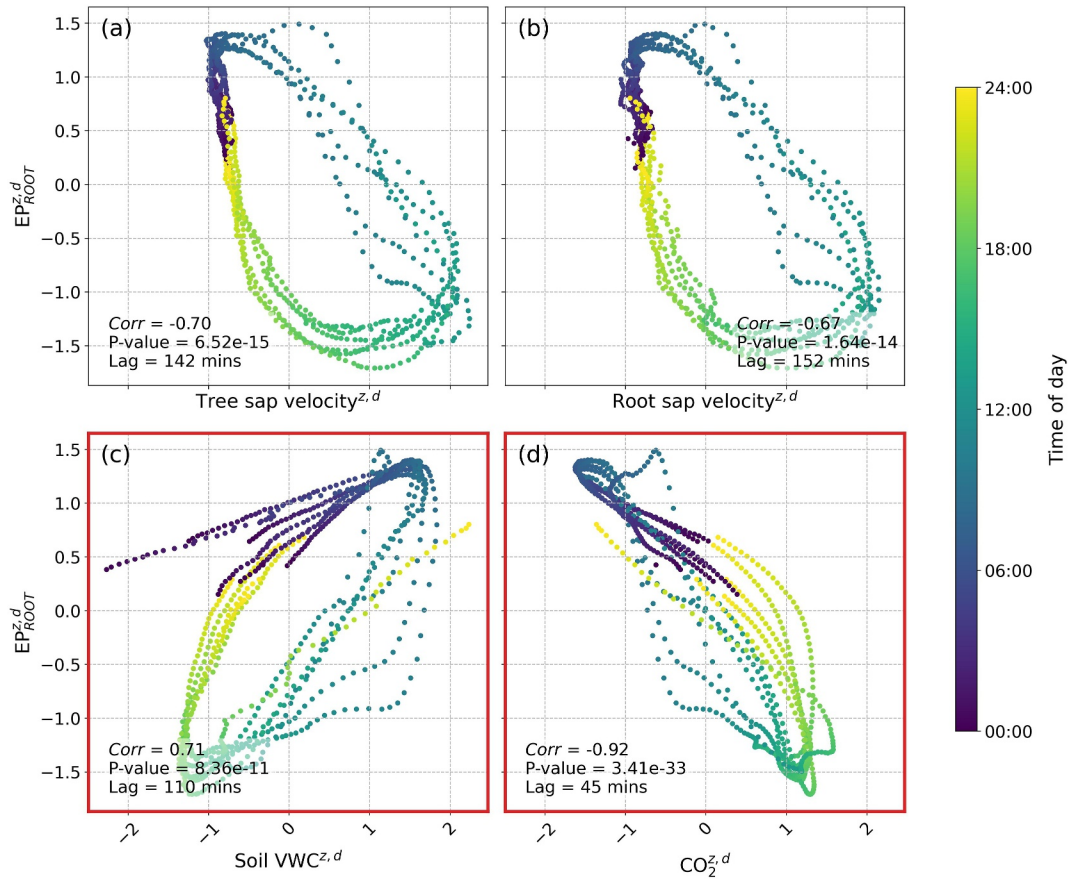

Figure 7. Daily correlation scatter plots of $EP_{ROOT}^{z,d}$ with (a) tree sap velocity, (b) root sap velocity, (c) soil water content, and (d) CO_2. The z-scored data presented here are unitless. The most significant time correlations are highlighted by red borders. Seasonal trends were removed from the data using a linear regression, and the data were then averaged weekly and normalized with a z-score to focus on the daily dynamics.

constraint, similar to sap-flow probes, arises from sapwood wounding around the screw interface, which quickly modifies wood properties around the electrode after the installation (Green et al., 2003). Another limitation is our focus on electrokinetic and redox sources, under the assumption that ion diffusion is limited in low-saturation soils. While Doro et al. (2022) and (Liu et al., 2022) reported large SP signals associated with microbial activity in the soil, Niu and McDavid (2025) showed that, under low water-flux conditions, electro-diffusive sources might dominate the SP signal. New laboratory experiments generating ionic diffusion and redox-related sources in a low-saturated soil would help to identify the dominant origin of the SP signal.

This work provides an important first step to untangle ecohydrological and biogeochemical interplays with passive electrical monitoring. Moving ahead, SP and EP measurements could be applied in different tree and forest types and combined with measurements of water fluxes, in the tree and the soil, and biogeochemical reactions, such as redox measurements. Such a setup could help to capture the interplay of water fluxes and biogeochemical reactions in the soil-tree continuum. For instance, our findings suggest that wildfire smoke had a stronger effect on soil respiration than tree transpiration. While trees maintain a certain level of transpiration, the reduced solar radiation may have muted daily air and soil temperature changes, reducing soil respiration.

Going forward, laboratory or greenhouse experiments might allow for parsing the exact controls on the signals and generate a more holistic model of the EP and SP signals. In trees, a quantitative interpretation of EP signals requires distinguishing the electrokinetic contribution associated with sap fluxes from electrochemical variations linked to diel changes in xylem and phloem solute concentrations. One promising avenue is the combined use of electrodes composed of a single metal type with concurrent sap electrical-conductivity measurements. Ion-selective electrodes, especially calcium- and potassium-selective ones (Hernández et al., 2010), could capture

ionic-activity variations in the tree in response to water stress and climatic forcing. Another opportunity would be the development of small non-polarizable electrodes to monitor SP signals in the tree and the roots over the growing season. They would only capture electrokinetic signals, allowing one to extract electrokinetic signals from EP measurements. In the soil, greenhouse monitoring of soil redox activity, soil moisture content and solute mineralization would help disentangle electrokinetic, redox, and electrochemical signals in a biologically active soil. The development of these tools could ultimately support our understanding of how climatic forcing influences water availability for trees, their physiological responses, and the biogeochemical dynamics of forest soils.

Conflict of Interest

The authors declare no conflicts of interest relevant to this study.

Data Availability Statement

Dumont and Singha (2026). Data from Dumont et al. (2026). Self- and Electrodic-Potential Response to Hydrological and Biogeochemical Processes in the Soil-Tree Continuum. HydroShare, http://www.hydroshare.org/resource/da9436b0422d4902911f41b405f5dbba.

Acknowledgments
This work is supported by the Department of Energy Grant DE-SC0023312, and the National Science Foundation EAR-2121659, EAR-2305616, and GRFP-2234662. H.J. Andrews Experiment Forest data and facilities were provided by the H.J. Andrews Experimental Forest and Long-Term Ecological Research program, administered cooperatively by Oregon State University, the USDA Forest Service Pacific Northwest Research Station, and the Willamette National Forest. This material is based upon work supported by the National Science Foundation under the Grant LTER8 DEB-2025755. We thank Luke Jacobsen, Josiah Chan, Katie Kusold, Fiona Liu, and H.J. Andrews team for their help in installing and maintaining the field experimentation, especially during a difficult fire season. Any opinion, findings, and conclusions or recommendations expressed in this material are those of the authors and do not necessarily reflect the views of the National Science Foundation. Open access publishing facilitated by Universite de Lausanne, as part of the Wiley - Universite de Lausanne agreement via the Consortium Of Swiss Academic Libraries.

References

Abatzoglou, J. T., & Williams, A. P. (2016). Impact of anthropogenic climate change on wildfire across western US forests. *Proceedings of the National Academy of Sciences*, *113*(42), 11770–11775. https://doi.org/10.1073/pnas.1607171113

Affortit, P., Ahmed, M. A., Grondin, A., Delzon, S., Carminati, A., & Laplaze, L. (2024). Keep in touch: The soil–root hydraulic continuum and its role in drought resistance in crops. *Journal of Experimental Botany*, *75*(2), 584-593–593. https://doi.org/10.1093/jxb/erad312

Arora, T., Linde, N., Revil, A., & Castermant, J. (2007). Non-intrusive characterization of the redox potential of landfill leachate plumes from self-potential data. *Journal of Contaminant Hydrology*, *92*(3–4), 274–292. https://doi.org/10.1016/j.jconhyd.2007.01.018

Atekwana, E. A., & Slater, L. D. (2009). Biogeophysics: A new Frontier in Earth science research. *Reviews of Geophysics*, *47*(4). https://doi.org/10.1029/2009RG000285

Attia al Hagrey, S. (2007). Geophysical imaging of root-zone, trunk, and moisture heterogeneity. *Journal of Experimental Botany*, *58*(4), 839-854–854. https://doi.org/10.1093/jxb/erl237

Ben-Noah, I., & Friedman, S. P. (2018). Review and evaluation of root respiration and of natural and agricultural processes of soil aeration. *Vadose Zone Journal*, *17*(1), 170119–170147. https://doi.org/10.2136/vzj2017.06.0119

Bigalke, J., & Grabner, E. W. (1997). The Geobattery model: A contribution to large scale electrochemistry. *Electrochimica Acta*, *42*(23), 3443–3452. https://doi.org/10.1016/S0013-4686(97)00053-4

Bond-Lamberty, B., Wang, C., & Gower, S. T. (2004). A global relationship between the heterotrophic and autotrophic components of soil respiration? *Global Change Biology*, *10*(10), 1756-1766. https://doi.org/10.1111/j.1365-2486.2004.00816.x

Bowman, M. M., Heath, A. E., Varga, T., Battu, A. K., Chu, R. K., Toyoda, J., et al. (2023). One thousand soils for molecular understanding of belowground carbon cycling. *Frontiers in Soil Science*, *3*, 1120425. https://doi.org/10.3389/fsoil.2023.1120425

Brantley, S. L., Goldhaber, M. B., & Ragnarsdottir, K. V. (2007). Crossing disciplines and scales to understand the critical zone. *Elements*, *3*(5), 307–314. https://doi.org/10.2113/gselements.3.5.307

Buckley, T. N. (2019). How do stomata respond to water status? *New Phytologist*, *224*(1), 21-36–36. https://doi.org/10.1111/nph.15899

Burgess, S. S. O., Adams, M. A., Turner, N. C., Beverly, C. R., Ong, C. K., Khan, A. A. H., & Bleby, T. M. (2001). An improved heat pulse method to measure low and reverse rates of sap flow in woody plants. *Tree Physiology*, *21*(9), 589–598. https://doi.org/10.1093/treephys/21.9.589

Callahan, R. P., Riebe, C. S., Sklar, L. S., Pasquet, S., Ferrier, K. L., Hahm, W. J., et al. (2022). Forest vulnerability to drought controlled by bedrock composition. *Nature Geoscience*, *15*(9), 714–719. https://doi.org/10.1038/s41561-022-01012-2

Campbell, G. S. (1988). Soil water potential measurement: An overview. *Irrigation Science*, *9*(4), 265–273. https://doi.org/10.1007/BF00296702

Carminati, A., Vetterlein, D., Koebernick, N., Blaser, S., Weller, U., & Vogel, H.-J. (2013). Do roots mind the gap? *Plant and Soil*, *367*(1), 651–661. https://doi.org/10.1007/s11104-012-1496-9

Carminati, A., Zarebanadkouki, M., Kroener, E., Ahmed, M. A., & Holz, M. (2016). Biophysical rhizosphere processes affecting root water uptake. *Annals of Botany*, *118*(4), 561–571. https://doi.org/10.1093/aob/mcw113

Chen, X., Gao, J., Zhao, P., McCarthy, H. R., Zhu, L., Ni, G., & Ouyang, L. (2018). Tree species with photosynthetic stems have greater nighttime sap flux. *Frontiers in Plant Science*, *9*, 30. https://doi.org/10.3389/fpls.2018.00030

Choi, W.-G., Miller, G., Wallace, I., Harper, J., Mittler, R., & Gilroy, S. (2017). Orchestrating rapid long-distance signaling in plants with Ca2+, ROS and electrical signals. *The Plant Journal*, *90*(4), 698–707. https://doi.org/10.1111/tpj.13492

Choi, W.-G., Toyota, M., Kim, S.-H., Hilleary, R., & Gilroy, S. (2014). Salt stress-induced Ca2+ waves are associated with rapid, long-distance root-to-shoot signaling in plants. *Proceedings of the National Academy of Sciences*, *111*(17), 6497–6502. https://doi.org/10.1073/pnas.1319955111

Christmann, A., Weiler, E. W., Steudle, E., & Grill, E. (2007). A hydraulic signal in root-to-shoot signalling of water shortage. *The Plant Journal*, *52*(1), 167-174–174. https://doi.org/10.1111/j.1365-313X.2007.03234.x

Cooper, W. T., Chanton, J. C., D'Andrilli, J., Hodgkins, S. B., Podgorski, D. C., Stenson, A. C., et al. (2022). A history of molecular level analysis of natural organic matter by FTICR mass spectrometry and the paradigm shift in organic geochemistry. *Mass Spectrometry Reviews*, *41*(2), 215–239. https://doi.org/10.1002/mas.21663

Cseresnyés, I., Takács, T., & Füzy, A. (2024). Detection of plant cadmium toxicity by monitoring dielectric response of intact root systems on a fine timescale. *Environmental Science and Pollution Research*, *31*(21), 30555–30568. https://doi.org/10.1007/s11356-024-33279-w

Daly, C., & Rothacher, J. S. (2025). Precipitation measurements from historic and current standard, storage and recording rain gauges at the Andrews Experimental Forest, 1951 to present [Dataset]. *Environmental Data Initiative*. https://doi.org/10.6073/pasta/6022898a200f7fac09aa36e79e0e66d7

Daly, C., Schulze, M. D., & McKee, W. A. (2025). *Meteorological data from benchmark stations at the HJ Andrews Experimental Forest, 1957 to present ver 37*. Environmental Data Initiative. https://doi.org/10.6073/pasta/5d4ab4b210165d6e860ebe58e0579e4e

DiDonato, N., Rivas-Ubach, A., Kew, W., Sokol, N. W., Clendinen, C. S., Kyle, J. E., et al. (2024). Improved characterization of soil organic matter by integrating FT-ICR MS, liquid chromatography tandem mass spectrometry, and molecular networking: A case study of root litter decay under drought conditions. *Analytical Chemistry*, *96*(29), 11699–11706. https://doi.org/10.1021/acs.analchem.4c00184

Dietz, K.-J., Turkan, I., & Krieger-Liszkay, A. (2016). Redox- and reactive oxygen species-dependent signaling into and out of the photosynthesizing chloroplast. *Plant Physiology*, *171*(3), 1541-1550–1550. https://doi.org/10.1104/pp.16.00375

Doro, K. O., Stoikopoulos, N. P., Bank, C.-G., & Ferris, F. G. (2022). Self-potential time series reveal emergent behavior in soil organic matter dynamics. *Scientific Reports*, *12*(1), 13531. https://doi.org/10.1038/s41598-022-17914-5

Dumont, M., & Singha, K. (2026). Self- and electrodic-potential response to hydrological and biogeochemical processes in the soil-tree continuum. *HydroShare*. http://www.hydroshare.org/resource/da9436b0422d4902911f41b405f5dbba

Ehosioke, S., Garré, S., Huisman, J. A., Zimmermann, E., Placencia-Gomez, E., Javaux, M., & Nguyen, F. (2023). Spectroscopic approach toward unraveling the electrical signature of roots. *Journal of Geophysical Research: Biogeosciences*, *128*(4), e2022JG007281. https://doi.org/10.1029/2022JG007281

Evett, S. R., Schwartz, R. C., Tolk, J. A., & Howell, T. A. (2009). Soil profile water content determination: Spatiotemporal variability of electromagnetic and neutron probe sensors in access tubes. *Vadose Zone Journal*, *8*(4), 926–941. https://doi.org/10.2136/vzj2008.0146

Fachin, S. J. S., Abreu, E. L., Mendonça, C. A., Revil, A., Novaes, G. C., & Vasconcelos, S. S. (2012). Self-potential signals from an analog biogeobattery model. *Geophysics*, *77*(4), EN29-EN37. https://doi.org/10.1190/geo2011-0352.1

Fernández, J. E., Palomo, M. J., Díaz-Espejo, A., Clothier, B. E., Green, S. R., Girón, I. F., & Moreno, F. (2001). Heat-pulse measurements of sap flow in olives for automating irrigation: Tests, root flow and diagnostics of water stress. *Agricultural Water Management*, *51*(2), 99-123. https://doi.org/10.1016/S0378-3774(01)00119-6

Forster, M. A. (2014). How significant is nocturnal sap flow? *Tree Physiology*, *34*(7), 757–765. https://doi.org/10.1093/treephys/tpu051

Foyer, C. H., & Noctor, G. (2005). Oxidant and antioxidant signalling in plants: A re-evaluation of the concept of oxidative stress in a physiological context. *Plant, Cell and Environment*, *28*(8), 1056-1071–1071. https://doi.org/10.1111/j.1365-3040.2005.01327.x

Gaupels, F., Durner, J., & Kogel, K.-H. (2017). Production, amplification and systemic propagation of redox messengers in plants? The phloem can do it all. *New Phytologist*, *214*(2), 554–560. https://doi.org/10.1111/nph.14399

Ghildiyal, V., Altaner, C. M., Heffernan, B., & Jarvis, M. C. (2025). Electrical phenomena in trees and wood: A review. *Current Forestry Reports*, *11*(1). https://doi.org/10.1007/s40725-024-00238-0

Gindl, W., Loppert, H., & Wimmer, R. (1999). Relationship between streaming potential and sap velocity in *Salix alba* L. *Phyton-Horn*, *39*, 217–224.

Gosling, S. N., & Arnell, N. W. (2016). A global assessment of the impact of climate change on water scarcity. *Climatic Change*, *134*(3), 371–385. https://doi.org/10.1007/s10584-013-0853-x

Green, S., Clothier, B., & Jardine, B. (2003). Theory and practical application of heat pulse to measure sap flow. *Agronomy Journal*, *95*(6), 1371-1379–1379. https://doi.org/10.2134/agronj2003.1371

Guo, Y., Cui, Y., Zhang, C., Xie, J., Zhang, P., Zhang, L., et al. (2024). Time-lapse self-potential signals from microbial processes: A laboratory perspective. *Journal of Applied Geophysics*, *228*, 105448. https://doi.org/10.1016/j.jappgeo.2024.105448

Guyot, A., Ostergaard, K. T., Lenkopane, M., Fan, J., & Lockington, D. A. (2013). Using electrical resistivity tomography to differentiate sapwood from heartwood: Application to conifers. *Tree Physiology*, *33*(2), 187–194. https://doi.org/10.1093/treephys/tps128

Hanson, P. J., Edwards, N. T., Garten, C. T., & Andrews, J. A. (2000). Separating root and soil microbial contributions to soil respiration: A review of methods and observations. *Biogeochemistry*, *48*(1), 115-146–146. https://doi.org/10.1023/A:1006244819642

Harmon, R. E., Barnard, H. R., Day-Lewis, F. D., Mao, D., & Singha, K. (2021). Exploring environmental factors that drive diel variations in tree water storage using wavelet analysis. *Frontiers in Water*, *3*, 682285. https://doi.org/10.3389/frwa.2021.682285

Harr, R. D., & McCorison, F. M. (1979). Initial effects of clearcut logging on size and timing of peak flows in a small watershed in western Oregon. *Water Resources Research*, *15*(1), 90–94. https://doi.org/10.1029/WR015i001p00090

Hermans, T., Nguyen, F., Robert, T., & Revil, A. (2014). Geophysical methods for monitoring temperature changes in shallow low enthalpy geothermal systems. *Energies*, *7*(8), 5083–5118. https://doi.org/10.3390/en7085083

Hernández, R., Riu, J., & Rius, F. X. (2010). Determination of calcium ion in sap using carbon nanotube-based ion-selective electrodes. *The Analyst*, *135*(8), 1979. https://doi.org/10.1039/c0an00148a

Hogg, E. H., & Hurdle, P. A. (1997). Sap flow in trembling aspen: Implications for stomatal responses to vapor pressure deficit. *Tree Physiology*, *17*(8–9), 501–509. https://doi.org/10.1093/treephys/17.8-9.501

Hölttä, T., Vesala, T., Sevanto, S., Perämäki, M., & Nikinmaa, E. (2006). Modeling xylem and phloem water flows in trees according to cohesion theory and Münch hypothesis. *Trees*, *20*(1), 67–78. https://doi.org/10.1007/s00468-005-0014-6

Hu, K., Jougnot, D., Huang, Q., Looms, M. C., & Linde, N. (2020). Advancing quantitative understanding of self-potential signatures in the critical zone through long-term monitoring. *Journal of Hydrology*, *585*, 124771. https://doi.org/10.1016/j.jhydrol.2020.124771

Hu, K., Loiseau, B., Carrière, S. D., Lesparre, N., Champollion, C., Martin-StPaul, N. K., et al. (2025). Self-potential signals related to tree transpiration in a Mediterranean climate. *Hydrology and Earth System Sciences*, *29*(13), 2997-3018. https://doi.org/10.5194/hess-29-2997-2025

Huber, A. E., & Bauerle, T. L. (2016). Long-distance plant signaling pathways in response to multiple stressors: The gap in knowledge. *Journal of Experimental Botany*, *67*(7), 2063-2079–2079. https://doi.org/10.1093/jxb/erw099

Husson, O. (2013). Redox potential (Eh) and pH as drivers of soil/plant/microorganism systems: A transdisciplinary overview pointing to integrative opportunities for agronomy. *Plant and Soil*, *362*(1), 389-417–417. https://doi.org/10.1007/s11104-012-1429-7

Jardani, A., Revil, A., Santos, F., Fauchard, C., & Dupont, J. p. (2007). Detection of preferential infiltration pathways in sinkholes using joint inversion of self-potential and EM-34 conductivity data. *Geophysical Prospecting*, *55*(5), 749–760. https://doi.org/10.1111/j.1365-2478.2007.00638.x

Javot, H., & Maurel, C. (2002). The role of aquaporins in root water uptake. *Annals of Botany*, *90*(3), 301–313. https://doi.org/10.1093/aob/mcf199

Joshi, J., Stocker, B. D., Hofhansl, F., Zhou, S., Dieckmann, U., & Prentice, I. C. (2022). Towards a unified theory of plant photosynthesis and hydraulics. *Nature Plants*, *8*(11), 1304–1316. https://doi.org/10.1038/s41477-022-01244-5

Jougnot, D., & Linde, N. (2013). Self-potentials in partially saturated media: The importance of explicit modeling of electrode effects. *Vadose Zone Journal*, *12*(2), vzj2012.0169. https://doi.org/10.2136/vzj2012.0169

Jougnot, D., Linde, N., Revil, A., & Doussan, C. (2012). Derivation of soil-specific streaming potential electrical parameters from hydrodynamic characteristics of partially saturated soils. *Vadose Zone Journal*, *11*(1), vzj2011.0086. https://doi.org/10.2136/vzj2011.0086

Kirwan, M. L., & Gedan, K. B. (2019). Sea-level driven land conversion and the formation of ghost forests. *Nature Climate Change*, *9*(6), 450–457. https://doi.org/10.1038/s41558-019-0488-7

Lassen, L. E., & Okkonen, E. A. (1969). Sapwood thickness of douglas-Fir and five other Western softwoods. *U.S.D.A. Forest Service Research Paper*.

Levengood, W. C. (1970). Redox currents associated with ion mobility in stems of plants. *Canadian Journal of Botany*, *48*(6), 1099–1108. https://doi.org/10.1139/b70-159

Liu, X., Zhang, Z., & Furman, A. (2022). Numerical modeling of physical and biochemical processes in the subsurface and their impacts on the self-potential signature. *Hydrology and Earth System Sciences Discussions*, *1–42*. https://doi.org/10.5194/hess-2022-31

Loiseau, B., Carrière, S. D., Jougnot, D., Singha, K., Mary, B., Delpierre, N., et al. (2023). The geophysical toolbox applied to forest ecosystems – A review. *Science of The Total Environment*, *899*, 165503. https://doi.org/10.1016/j.scitotenv.2023.165503

Mares, R., Barnard, H. R., Mao, D., Revil, A., & Singha, K. (2016). Examining diel patterns of soil and xylem moisture using electrical resistivity imaging. *Journal of Hydrology*, *536*, 327-338–338. https://doi.org/10.1016/j.jhydrol.2016.03.003

Marshall, D. C. (1958). Measurement of sap flow in conifers by heat transport. 1. *Plant Physiology*, *33*(6), 385–396. https://doi.org/10.1104/pp.33.6.385

Mattila, T. J. (2024). Redox potential as a soil health indicator—How does it compare to microbial activity and soil structure? *Plant and Soil*, *494*(1), 617–625. https://doi.org/10.1007/s11104-023-06305-y

McGuire, K. J., Weiler, M., & McDonnell, J. J. (2007). Integrating tracer experiments with modeling to assess runoff processes and water transit times. *Advances in Water Resources*, *30*(4), 824-837–837. https://doi.org/10.1016/j.advwatres.2006.07.004

Merlin, M., Solarik, K. A., & Landhäusser, S. M. (2020). Quantification of uncertainties introduced by data-processing procedures of sap flow measurements using the cut-tree method on a large mature tree. *Agricultural and Forest Meteorology*, *287*, 107926. https://doi.org/10.1016/j.agrformet.2020.107926

Miele, F., Benettin, P., Wang, S., Retti, I., Asadollahi, M., Frutschi, M., et al. (2023). Spatially explicit linkages between redox potential cycles and soil moisture fluctuations. *Water Resources Research*, *59*(3), e2022WR032328. https://doi.org/10.1029/2022WR032328

Miller, G., Shulaev, V., & Mittler, R. (2008). Reactive oxygen signaling and abiotic stress. *Physiologia Plantarum*, *133*(3), 481-489–489. https://doi.org/10.1111/j.1399-3054.2008.01090.x

Nadezhdina, N., David, T. S., David, J. S., Ferreira, M. I., Dohnal, M., Tesař, M., et al. (2010). Trees never rest: The multiple facets of hydraulic redistribution. *Ecohydrology*, *3*(4), 431–444. https://doi.org/10.1002/eco.148

Nawrath, C., Schreiber, L., Franke, R. B., Geldner, N., Reina-Pinto, J. J., & Kunst, L. (2013). Apoplastic diffusion barriers in arabidopsis. *The Arabidopsis Book / American Society of Plant Biologists*, *11*, e0167. https://doi.org/10.1199/tab.0167

Neumann, R. B., & Cardon, Z. G. (2012). The magnitude of hydraulic redistribution by plant roots: A review and synthesis of empirical and modeling studies. *New Phytologist*, *194*(2), 337–352. https://doi.org/10.1111/j.1469-8137.2012.04088.x

Niu, Q., & McDavid, C. (2025). Self-potential signals of soil columns experiencing evaporation and transpiration. *Vadose Zone Journal*, *24*(2), e70009. https://doi.org/10.1002/vzj2.70009

Ojo, E. R., Bullock, P. R., L'Heureux, J., Powers, J., McNairn, H., & Pacheco, A. (2015). Calibration and evaluation of a frequency domain reflectometry sensor for real-time soil moisture monitoring. *Vadose Zone Journal*, *14*(3), vzj2014-08. https://doi.org/10.2136/vzj2014.08.0114

Peláez-Vico, M. Á., Fichman, Y., Zandalinas, S. I., Van Breusegem, F., Karpiński, S. M., & Mittler, R. (2022). ROS and redox regulation of cell-to-cell and systemic signaling in plants during stress. *Free Radical Biology and Medicine*, *193*, 354–362. https://doi.org/10.1016/j.freeradbiomed.2022.10.305

Personna, Y. R., Ntarlagiannis, D., Slater, L., Yee, N., O'Brien, M., & Hubbard, S. (2008). Spectral induced polarization and electrodic potential monitoring of microbially mediated iron sulfide transformations. *Journal of Geophysical Research*, *113*(G2). https://doi.org/10.1029/2007JG000614

Peruzzo, L., Liu, X., Chou, C., Blancaflor, E. B., Zhao, H., Ma, X.-F., et al. (2021). Three-channel electrical impedance spectroscopy for field-scale root phenotyping. *The Plant Phenome Journal*, *4*(1), e20021. https://doi.org/10.1002/ppj2.20021

Peters, R. L., Miranda, J. C., Schönbeck, L., Nievergelt, D., Fonti, M. V., Saurer, M., et al. (2020). Tree physiological monitoring of the 2018 larch budmoth outbreak: Preference for leaf recovery and carbon storage over stem wood formation in Larix decidua. *Tree Physiology*, *40*(12), 1697–1711. https://doi.org/10.1093/treephys/tpaa087

Petiau, G. (2000). Second generation of lead-lead chloride electrodes for geophysical applications. *Pure and Applied Geophysics*, *157*(3), 357–382. https://doi.org/10.1007/s000240050004

Raich, J. W. (1998). Aboveground productivity and soil respiration in three Hawaiian rain forests. *Forest Ecology and Management*, *107*(1), 309–318. https://doi.org/10.1016/S0378-1127(97)00347-2

Raich, J. W., & Tufekciogul, A. (2000). Vegetation and soil respiration: Correlations and controls. *Biogeochemistry*, *48*(1), 71–90. https://doi.org/10.1023/A:1006112000616

Revil, A., & Jardani, A. (2013). *The self-potential method: Theory and applications in environmental geosciences*. Cambridge University Press.

Revil, A., Mendonça, C. A., Atekwana, E. A., Kulessa, B., Hubbard, S. S., & Bohlen, K. J. (2010). Understanding biogeobatteries: Where geophysics meets microbiology. *Journal of Geophysical Research*, *115*(G1). https://doi.org/10.1029/2009JG001065

Revil, A., Meyer, C. D., & Niu, Q. (2016). A laboratory investigation of the thermoelectric effect. *Geophysics*, *81*(4), E243-E257–E257. https://doi.org/10.1190/geo2015-0281.1

Rittgers, J. B., Revil, A., Karaoulis, M., Mooney, M. A., Slater, L. D., & Atekwana, E. A. (2013). Self-potential signals generated by the corrosion of buried metallic objects with application to contaminant plumes. *Geophysics*, *78*(5), EN65–EN82. https://doi.org/10.1190/geo2013-0033.1

Ros-Barceló, A., Gómez-Ros, L. V., Ferrer, M. A., & Hernández, J. A. (2006). The apoplastic antioxidant enzymatic system in the wood-forming tissues of trees. *Trees*, *20*(2), 145–156. https://doi.org/10.1007/s00468-005-0020-8

Sato, M., & Mooney, H. M. (1960). The electrochemical mechanism of sulfide self-potentials. *Geophysics*, *25*(1), 226–249. https://doi.org/10.1190/1.1438689

Scheibe, R., Backhausen, J. E., Emmerlich, V., & Holtgrefe, S. (2005). Strategies to maintain redox homeostasis during photosynthesis under changing conditions. *Journal of Experimental Botany*, *56*(416), 1481–1489. https://doi.org/10.1093/jxb/eri181

Sevanto, S., Nikinmaa, E., Riikonen, A., Daley, M., Pettijohn, J. C., Mikkelsen, T. N., et al. (2008). Linking xylem diameter variations with sap flow measurements. *Plant and Soil*, *305*(1), 77-90–90. https://doi.org/10.1007/s11104-008-9566-8

Slater, L., Ntarlagiannis, D., Yee, N., O'Brien, M., Zhang, C., & Williams, K. H. (2008). Electrodic voltages in the presence of dissolved sulfide: Implications for monitoring natural microbial activity. *Geophysics*, *73*(2), F65–F70. https://doi.org/10.1190/1.2828977

Soldi, M., Jougnot, D., & Guarracino, L. (2018). An analytical effective excess charge density model to predict the streaming potential generated by unsaturated flow. *Geophysical Journal International*, *216*(1). https://doi.org/10.1093/gji/ggy391

Spaans, E. J. A., & Baker, J. M. (1992). Calibration of watermark soil moisture sensors for soil matric potential and temperature. *Plant and Soil*, *143*(2), 213–217. https://doi.org/10.1007/BF00007875

Szechyńska-Hebda, M., Kruk, J., Górecka, M., Karpińska, B., & Karpiński, S. (2010). Evidence for light wavelength-specific photoelectrophysiological signaling and memory of excess light episodes in arabidopsis. *The Plant Cell*, *22*(7), 2201-2218. https://doi.org/10.1105/tpc.109.069302

Tattar, T. A., & Blanchard, R. O. (1976). Electrophysiological research in plant pathology. *Annual Review of Phytopathology*, *14*(1), 309–325. https://doi.org/10.1146/annurev.py.14.090176.001521

Teshome, D. T., Zharare, G. E., & Naidoo, S. (2020). The threat of the combined effect of biotic and abiotic stress factors in forestry under a changing climate. *Frontiers in Plant Science*, *11*, 601009. https://doi.org/10.3389/fpls.2020.601009

Tokunaga, T. K., Finsterle, S., Kim, Y., Wan, J., Lanzirotti, A., & Newville, M. (2017). Ion diffusion within water films in unsaturated porous media. *Environmental Science & Technology*, *51*(8), 4338–4346. https://doi.org/10.1021/acs.est.6b05891

Venturas, M. D., Sperry, J. S., & Hacke, U. G. (2017). Plant xylem hydraulics: What we understand, current research, and future challenges. *Journal of Integrative Plant Biology*, *59*(6), 356–389. https://doi.org/10.1111/jipb.12534

Voytek, E. B., Barnard, H. R., Jougnot, D., & Singha, K. (2019). Transpiration- and precipitation-induced subsurface water flow observed using the self-potential method. *Hydrological Processes*, *33*(13), 1784–1801. https://doi.org/10.1002/hyp.13453

Walker, J. P., Willgoose, G. R., & Kalma, J. D. (2004). In situ measurement of soil moisture: A comparison of techniques. *Journal of Hydrology*, *293*(1), 85-99–99. https://doi.org/10.1016/j.jhydrol.2004.01.008

Wang, H., Guan, H., Guyot, A., Simmons, C. T., & Lockington, D. A. (2016). Quantifying sapwood width for three Australian native species using electrical resistivity tomography. *Ecohydrology*, *9*(1), 83–92. https://doi.org/10.1002/eco.1612

Williams, A., & de Vries, F. T. (2020). Plant root exudation under drought: Implications for ecosystem functioning. *New Phytologist*, *225*(5), 1899–1905. https://doi.org/10.1111/nph.16223

Yang, Y., Patel, R. A., Prasianakis, N. I., Churakov, S. V., Deissmann, G., & Bosbach, D. (2024). Elucidating the role of water films on solute diffusion in unsaturated porous media by improved pore-scale modeling. *Vadose Zone Journal*, *23*(3), e20321. https://doi.org/10.1002/vzj2.20321

Zapata, R., Oliver-Villanueva, J.-V., Lemus-Zúñiga, L.-G., Fuente, D., Mateo Pla, M. A., Luzuriaga, J. E., & Moreno Esteve, J. C. (2021). Seasonal variations of electrical signals of Pinus halepensis mill. In mediterranean forests in dependence on climatic conditions. *Plant Signaling & Behavior*, *16*(10), 1948744. https://doi.org/10.1080/15592324.2021.1948744

Zapata, R., Oliver-Villanueva, J.-V., Lemus-Zúñiga, L.-G., Luzuriaga, J. E., Mateo Pla, M. A., & Urchueguía, J. F. (2020). Evaluation of electrical signals in pine trees in a mediterranean forest ecosystem. *Plant Signaling & Behavior*, *15*(10), 1795580. https://doi.org/10.1080/15592324.2020.1795580

Zhang, C., Ntarlagiannis, D., Slater, L., & Doherty, R. (2010). Monitoring microbial sulfate reduction in porous media using multipurpose electrodes. *Journal of Geophysical Research*, *115*(G3). https://doi.org/10.1029/2009JG001157

Zhang, Z., & Furman, A. (2021). Soil redox dynamics under dynamic hydrologic regimes—A review. *Science of The Total Environment*, *763*, 143026. https://doi.org/10.1016/j.scitotenv.2020.143026

Zhuang, Y., Zhu, G., Jin, Y., Qu, M., Lin, Q., & Zeng, L. (2024). Diffusion hysteresis in unsaturated porous media: A microfluidic study. *Journal of Hydrology*, *640*, 131675. https://doi.org/10.1016/j.jhydrol.2024.131675

Zimmermann, M. R., Maischak, H., Mithöfer, A., Boland, W., & Felle, H. H. (2009). System potentials, a novel electrical long-distance apoplastic signal in plants, induced by wounding. *Plant Physiology*, *149*(3), 1593–1600. https://doi.org/10.1104/pp.108.133884

Zlotnicki, J., & Nishida, Y. (2003). Review on morphological insights of self-potential anomalies on volcanoes. *Surveys in Geophysics*, *24*(4), 291–338. https://doi.org/10.1023/B:GEOP.0000004188.67923.ac